AALBORG UNIVERSITY
Department of Health Science and Technology

Phantom Limb Illusion: Loss of visual feedback modulates proprioceptive and cortical responses to somatosensory stimuli

Anastasia M. Galanopoulou, Magdalena Czyżewska

Project period: 01-09-2016 - 07-06-2017
Supervisor: Bo Geng
Co-supervisors: Federico Gabriel Arguissain, Mikkel Thøgersen
Group number: 17gr10401

Department of Health Science and Technology
Fredrik Bajers Vej 7 D2
DK-9220 Aalborg East
Denmark
Telephone: +45 9940 9940
Fax: +45 9815 4008
http://www.hst.aau.dk

AALBORG UNIVERSITY
DENMARK

Title: Phantom Limb Illusion: Loss of visual feedback modulates the proprioceptive and cortical responses to somatosensory stimuli

Theme: Phantom Limb Pain

Authors: Anastasia Maria Galanopoulou and Magdalena Czyżewska

Project period:
Project start: 01-09-2016
Project end: 07-06-2017

Supervisors:
Main supervisor: Bo Geng
Co-supervisors: Federico Gabriel Arguissain, Mikkel Thøgersen

Total no. of pages: 71
Completed: 06-06-2017

Summary:
This thesis investigates how the loss of visual feedback, created by a novel mixed reality system, modulates pain perception, proprioception and cortical responses to somatosensory stimulation. Cortical reorganisations and deafferentation after amputation are related to the phantom limb pain condition. However, the mechanisms behind PLP are still poorly understood. Intriguingly, visual feedback modulates pain perception, therefore its loss from the missing limb can contribute to PLP. The mixed reality system was used to create a phantom limb illusion in heathy participants creating a missing upper limb experience. Behavioural and electrophysiological data were obtained during different conditions (with and without the visual illusion) and analysed in order to investigate different effects. This thesis shows that the phantom limb illusion induced temporal changes on the cortical responses and proprioception. The results suggest the importance of visual feedback in phantom conditions. Further investigation is needed to show if this effect is unique to sensory processing or associated with more abstract cognitive processing. Furthermore, it is crucial to research if this illusion has a permanent effect rather than temporal.

Phantom Limb Illusion: Loss of visual feedback modulates proprioceptive and cortical responses to somatosensory stimuli

Magdalena Czyżewska, Anastasia Maria Galanopoulou
Aalborg University
mczyze15@student.aau.dk, agalan15@student.aau.dk

Abstract

Introduction: Deafferentation after amputation and consequent cortical reorganization have been associated with the phantom limb pain (PLP) condition. Still, the mechanisms behind PLP remain unclear. Interestingly, pain perception is altered by visual feedback. It could therefore be possible that the loss of visual feedback from the missing limb might contribute to the development of PLP. **Aim**: Investigate how missing visual feedback modulates pain perception, proprioception and cortical activity. **Methods**: A phantom limb illusion was created in twenty healthy participants by a novel mixed reality (MR) system to investigate the effect of loss of visual feedback. Electrophysiological and behavioral data were obtained by recording cortical responses evoked by electrical stimulation, collecting subjective pain ratings and measuring proprioception in three different conditions (control, illusion, covered). **Results**: There was a proprioceptive drift between illusion and control for the tip of the index finger ($p < 0.001$), knuckle ($p = 0.004$) and location of stimulation ($p = 0.014$). Additionally, larger cortical activity was observed within the parietal lobe during illusion when compared to the other conditions ($p < 0.001$). The subjective pain ratings showed no significant differences among conditions. **Discussion**: The results demonstrated that the phantom limb illusion modulates proprioception and cortical responses to somatosensory stimulation. These responses may not be unique to nociceptive stimulation but they may be evoked by saliency sensory processing.

Keywords: phantom limb pain, mixed reality, pain perception, proprioception, event-related potentials

I. Introduction

People who have undergone amputation, commonly report painful sensations from the phantom limb. This condition is known as phantom limb pain (PLP) [1]. PLP is a neuropathic chronic pain occuring in up to 50 - 85% of amputees [2, 3]. It has been suggested that one of the multiple mechanisms behind it is cortical reorganization in specific brain regions, particularly in the primary somatosensory cortex (SI) [4, 5].

Due to deafferentation, the inactive area representing the amputated limb is shrinking, whereas the neighboring areas are expanding into the inactive area [5]. These changes may affect the body schema. The body schema is modified dynamically by multiple inputs such as visual, proprioceptive and efferent; hence, changes such as amputation, can lead to phantom sensations [6, 7].

Not only is the body schema susceptible to visual feedback, but also pain perception seems to be influenced by altered visual feedback. Particularly, it has been shown that neuropathic chronic pain patients experienced an analgesic effect when they saw their body [8, 9]. Moreover, studies that implemented visual illusions have reported a reduction of pain [10, 11, 12]. For example in mirror therapy, the perception of pain is decreased when a person is looking at the reflection of the intact body part mirrored onto the position of the missing limb [10, 13, 14].

Apart from the illusions, simply seeing one's body instead of an object can reduce the perceived pain in healthy participants [15]. This does not only involve pain ratings but also cortical activity. Electroencephalography (EEG) and functional magnetic resonance imaging (fMRI) studies have shown that the amplitude of the cortical responses is lower while looking at one's hand instead of an object [12, 16].

However, it is still unclear whether the loss of visual feedback by itself can modulate the pain perception, proprioception and cortical responses. The aim of the present study is to investigate how the loss of visual feedback modulates the way a person perceives, localizes and responds to somatosensory stimulation. A phantom limb illusion was created in healthy participants by using a mixed reality (MR) system. The effect of loss of visual

feedback was tested by analyzing event related potentials (ERPs) evoked by electrical stimulation, pain intensity ratings and proprioceptive drift measures. It was hypothesized that during the illusion behavioral and cortical responses of healthy participants are modulated. Particularly, an enhanced pain perception and brain activity, and a drift in proprioception was expected.

II. Methods

Participants

Twenty participants (11 male and 9 female, aged 25.5 $\pm$ 4.16, age range 19-34) were enrolled in the experiment. Participants were recruited through personal inquiry and were naive to the aims of the study. All participants gave their informed written consent prior to the experiment. Due to the use of the MR system the exclusion criteria included: claustrophobia, nausea, blurry vision, tendency to get headaches and migraines. None of the participants had acknowledged neurological, musculoskeletal or mental disorders. The procedures were approved by the North Denmark Region Committee on Health Research Ethics (N-20160021) and were performed in accordance with the Declaration of Helsinki.

Electroencephalographic recordings

Electroencephalography was recorded with a standard 64-channel electrode cap based on the extended international 10-20 system. The ground electrode was placed along the sagittal mid-line between Fz and FCz electrodes and the reference was placed on the ear lobe. The cap was fixed tightly and gel was used to ensure good conductivity between the scalp and the electrodes. EEG data was filtered with a notch filter (50 Hz), sampled at 2048 Hz per channel and stored for offline analysis using g.HIamp multichannel amplifier (G.Tec Medical Engineering GMBH, Austria).

Electrical stimulation

A cutaneous pin electrode (CPE; custom made at Aalborg University, approved for research purposes) was placed at the participants' left forearm to deliver electrical stimulation [17]. The CPE electrode delivers a stimulation that is generally described as a sharp, pin pricking sensation [17]. Before placing the electrode the participants' skin was cleaned with alcohol and wiped with a paper towel in order to remove the dead cells of the epidermis. Next, the detection threshold was determined individually for each participant with single-pulse (4s) stimuli using the staircase procedure [18]. Subsequently, two different stimuli intensities were calculated based on detection threshold intensity (0.16 $\pm$ 0.06 mA): low intensity (0.32 $\pm$ 0.13 mA, twice the detection threshold) and high intensity (0.63 $\pm$ 0.25 mA, four times the detection threshold). The threshold detection and stimulation protocol where implemented using Mr. Kick © (SMI, Aalborg University 2000) a data acquisition software that controlled a constant current stimulator DS5 (Digitimer, Hertfordshire,UK).

Phantom Limb Illusion

The phantom limb illusion was created by removing the visual feedback with the use of a novel MR system developed by Thøgersen et al. [19]. This system allows for a more realistic and immersive experience than the conventional illusory methods. The design is based on green-screen technology with the use of the MR system. Two cameras attached to a Virtual Reality (VR) helmet feed pictures to the screens inside the VR device, creating a see-through device with the possibility of manipulating the participants' view. A picture is taken from the background in order to be used as the background itself and then the illusion is created by replacing everything green with the pre-captured background picture. Hence, placing a green glove on the participants' hand and arm renders the arm invisible to the participant.
The participants were seated on a chair with the left hand and arm placed face down on a table in front of them and their right hand was placed below the table resting on their lap. The participants' head was placed in the fixation array on which the mixed reality system was mounted, preventing the EEG cap electrodes to touch the device. The MR system was placed in a comfortable position for the participants so that it was held steady and tight to their face.

Experimental procedure

The experiment included three different conditions which aimed to test the effect of different visual inputs on the perception of pain and on ERPs evoked by somatosensory stimuli. The conditions were: control, illusion and covered.
In the control condition the participants were able to see and recognize the shape of their hand and forearm. However, they could not see the stimulation electrode because

it was attached to the side of the arm facing down on the table.
In the illusion condition the participants wore a green glove and the illusion procedure was applied to make the hand and forearm disappear from their view. During this procedure, the participants were asked to relax and focus on their hand and forearm while they listened to a recorded speech. The aim of the speech was to force the participants to keep their attention on their limb and thus, create the feeling of losing it. A fragment of the speech is: "I would like you to think of your left hand. Feel it. Now, it becomes numb and light, very light... You start to notice how your hand slowly begins to disappear... disappears and becomes nothing..." [19]. After the speech there were 2-3 minutes of silence in which the participants were asked to reflect on their experience.
In the covered condition the participants' hand and forearm were covered with a green towel. The covered part of the limb was the same as the missing part in the illusion condition. The participants could see their arm covered by the towel through the display. The texture of the towel was soft and was touching their hand and forearm directly. The participants took part in all three conditions which appeared in a counterbalanced order. They were connected to the mixed reality system and were looking through the head mounted display in all the conditions. The EEG data was recorded for each condition. The experimental procedure is shown in the figure 1.

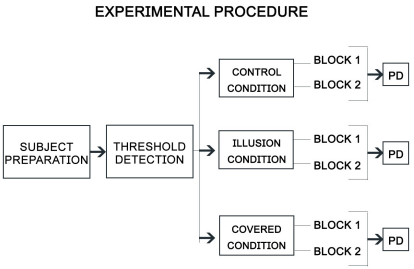

Figure 1: *The steps of the experimental procedure. PD indicates the proprioceptive drift measurements. The order of the conditions was counterbalanced in every experimental trial.*

For each experimental condition, somatosensory stimuli were delivered in two blocks of stimulation with an interval of 1-2 minutes between them. Every block consisted of 30 stimuli separated with randomized intervals which ranged between 8 and 12 seconds. The two different intensities were used in a counterbalanced order. After each stimulus the participants were asked to estimate the intensity of the stimulus on a 10-point visual analogue scale (VAS), where 0 means no pain and 10 means unbearable pain. In total, 60 stimuli were delivered in every condition resulting in 60 pain ratings.

Proprioceptive drift measures

A proprioceptive drift (PD) measure was conducted at the end of every condition. This measure was used before in several studies related to the rubber hand illusion [20, 21] and it is used "as a proprioceptive marker for the perception of the spatial layout of the body" [19]. The PD was measured with a slider located on the right side of the participants, under the table. The participants were asked to use the slider with their right hand to locate the position of four measured points relative to their left hand. The four measured points were: the tip of the index finder, the knuckle on the index finger root, the joint of the wrist and the location of stimulus [19]. The location of the stimulus was measured by delivering a single stimulation to the participants at the end of each condition and asking them to locate where they felt it. This was done to check if the localization of pain changes under different conditions. Two reference measures were taken afterwards from a fixed line on the table to the tip of the left index finger and to the center of the electrode on the forearm. During the measurements, the participants were instructed to keep their left hand still. Three repetitions of PD measures were conducted for every measured point in counterbalanced order. Additionally, the length of the index finger and the length between the knuckle and the wrist were measured for each participant in order to calculate the actual position of the measured points.

EEG data processing

The EEG data was processed using Matlab R2016b ® (MathWorks Inc., USA) with EEGLab toolbox [22]. Initially, the continuous EEG data was visually inspected for faulty and noisy channels which were removed from the data. Next, the data was filtered using a passband filter with a lower edge of 0.5 Hz and a higher edge of 40 Hz. Afterwards, the EEG data was segmented into 2-seconds epochs. An infomax independent component analysis

(ICA) was applied on the epochs for each condition, block and participant (3 x 60 x 20 ERPs for each electrode) using the 'runica' EEGLab algorithm. Subsequently, the independent components were visually inspected and the artefacts were removed. Following, the data was re-referenced to the average of all electrodes and an one second baseline was removed.

Statistical Analysis

For the statistical analysis, SPSS ® 24 (IBM Inc., USA) and Matlab R2016b ® (MathWorks Inc., USA) with Letswave tooldbox (http://www.nocions.org/letswave/) were used. Both VAS and PD data were checked for normality using Shapiro-Wilks tests. For the VAS data, the mean value for every condition and stimulus intensity was calculated per subject. To compare the intensity of pain perception among the three conditions a two-way repeated measures analysis of variance (ANOVA) was conducted with the factors condition (control, illusion and covered) and intensity (low vs high). The effect of the factor condition on the PD was analysed with one-way repeated measures ANOVA. Four different statistical tests were conducted for the dependent factors: the location of the tip of the index finger, the location of the knuckle, the location of the wrist and the location of the stimulation. For all the data the sphericity was assumed and for the PD data a paired t-test with Bonferroni correction was performed.
An one-way ANOVA was performed on the amplitudes and latencies of the ERP components with the factor condition only for high-intensity stimulation data. Additionally, a paired t-test with a cluster-based permutation was performed on each time point of the ERP waveforms to evaluate the time points where the ERP waveforms showed significant differences. The permutation test (250 random permutations of the conditions within all subjects) was used to determine the distribution of cluster magnitudes in randomly transferred data. A threshold for within-subject factors was set at the 95th percentile of the cluster magnitude distribution (i.e., p<.05). Applying this method allowed to find time intervals where the ERP waveforms had a significant effect of the factor condition.

III. Results

Subjective pain ratings

The two-way repeated measures ANOVA performed on the intensity of pain perception of somatosensory stimuli did not show significant differences among the three conditions ($F(2,0.147) = 0.864$, $p < 0.05$) or for the interaction of factors condition and intensity ($F(2,0.556) = 0.578$, $p < 0.05$). However, it showed significant differences between the two intensities ($F(1,75.158) = 0.000$, $p < 0.05$). The averaged values of the pain ratings with the standard deviation are shown in figure 2.

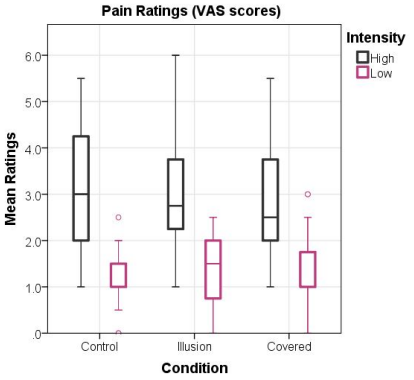

Figure 2: *The averaged values of subjective pain ratings for each condition for both intensities Outliers are plotted as the values outside of the boxplots.*

Proprioceptive drift

The average values for each measured point and for each condition is reported and shown in figure 3. The paired t-tests with Bonferroni corrections for control vs illusion, illusion vs covered and control vs covered conditions are reported and shown in figure 3. In general, participants reported that the position of the tip of the index finger was significantly more proximal to the actual position of the measured point during the control when compared to the illusion condition ($t(19) = -4.98$, $p < 0.0001$) and to covered condition ($t(19) = -2.71$, $p = 0.014$). Additionally, they reported that the position of the knuckle was significantly more proximal to the actual position of the measured point during the control condition comparing to the illusion ($t(19) = -3.28$, $p = 0.004$). Furthermore, they reported that the location of the stimulation was more distal from the actual position from the measured point during illusion compared to the control condition (t(19)

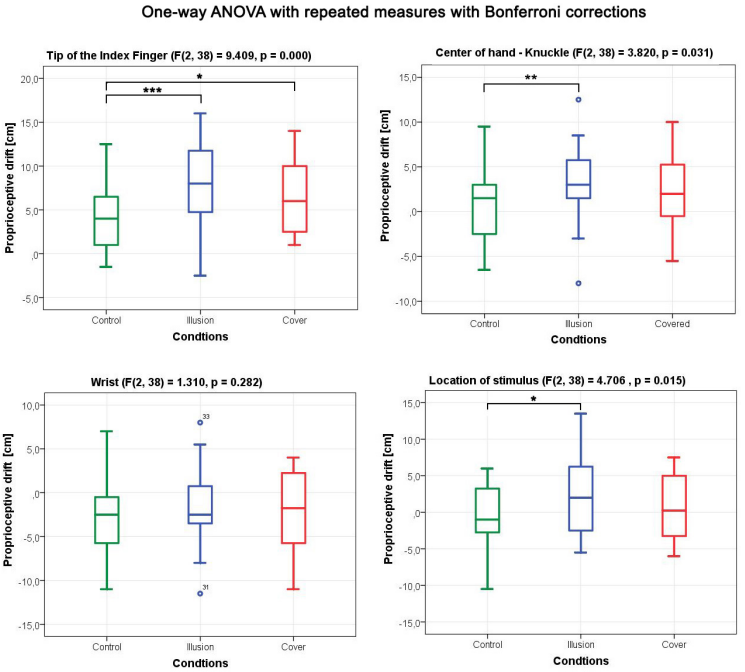

Figure 3: *The proprioceptive drift measure shows the difference between the actual position of measured point and the position determined by the participants. The plots show the averaged values for each conditions. One star(*) indicates that $p < 0.05$, two stars (**) indicate that $p < 0.01$ and three stars (***) indicate $p < 0.001$. Outliers are plotted as the values outside of the boxplots.*

= -2.7, p = 0.014).

Event-related potentials

The averaged values for latencies and amplitudes of the ERPs for each condition are shown in table 1 and in figure 4. One-way ANOVA with repeated measures with the factor condition was conducted on these data and the results are shown in table 2. The magnitude of ERPs during illusion was on average greater than the one during covered and control conditions. Moreover, there were significant differences on the amplitude for control vs illusion and illusion vs covered ($p < 0.001$). Furthermore, the results showed significant difference on the latency of the N-wave for control vs illusion and control vs covered.

The results of the point-by-point paired-sample t-test with cluster-based thresholding evaluating the effects of condition on the ERPs are shown in figure 5. Significant differences for control vs illusion and illusion vs covered were observed within central, parietal and occipital lobes, whereas for control vs covered within the occipital lobe. The significance was observed mainly in the contralateral side of the stimulated hand. Figure 5 displays only the results for the high-intensity stimulation and specific

Table 1: *Latencies and Amplitudes of the ERPs for each condition. N-wave indicates the negative peak, P-wave indicates the positive peak and SD = standard deviation.*

	Control		Illusion		Covered	
	Latency [mean ± SD (ms)]	Amplitude [mean ± SD (μV)]	Latency [mean ± SD (ms)]	Amplitude [mean ± SD (μV)]	Latency [mean ± SD (ms)]	Amplitude [mean ± SD (μV)]
N1-wave	108 ± 45	3.7 ± 1.9	111.7 ± 45	3.7 ± 1.8	110.5 ± 47	3.7 ± 1.9
P2-wave	279.8 ± 27	5.1 ± 3.1	284.5 ± 25	6.4 ± 3.3	271.9 ± 45	4.9 ± 2.8

Table 2: *The results of one-way ANOVA with repeated measures on the ERPs (amplitude and latency) with the factor condition. The significance level was set to 0.05. The pairs that showed significant differences after the test are indicated with the stars; *** means $p < 0.001$ and ** means $p < 0.01$.*

p values for ERPs						
	Control vs Illusion		Illusion vs Covered		Covered vs Control	
	P2-wave	N1-wave	P2-wave	N1-wave	P2-wave	N1-wave
Amplitude	0.000 ***	1.000	0.000 ***	1.000	0.252	1.000
Latency	0.155	0.000 ***	0.182	0.092	0.655	0.009 **

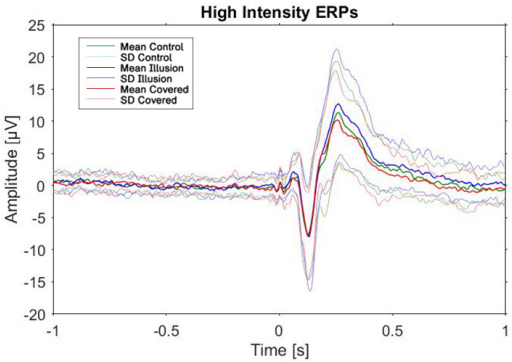

Figure 4: *The averaged ERPs with the standard deviation among the three conditions recorded at FCz electrode for high-intensity stimulation.*

electrodes are shown.

Particularly, participants presented a larger ERP in the illusion condition when compared to the control in ∼ 240-310 ms and ∼ 320-410 ms. Moreover, the ERP during illusion was also enhanced when compared to covered in ∼ 238-410 ms and ∼ 450-597 ms. These time windows are indicated by the shaded areas in figure 5.

Apart from the waveforms, the ERPs were also identified in scalp maps. In figure 6 they are displayed as topographic maps for control and illusion conditions at selected time points with the p values shown in the last row of the graph.

IV. Discussion

The aim of the study was to create a missing limb illusion in healthy participants and investigate if the loss of visual feedback can modulate pain perception, proprioception and cortical responses to nociceptive stimulation. The results showed that the illusion caused a mismatch in localization and also an increase in cortical activity. This indicates that the absence of visual feedback alone can alter the body representation in healthy subjects and also the way they respond to somatosensory stimuli in regards to cortical activity.

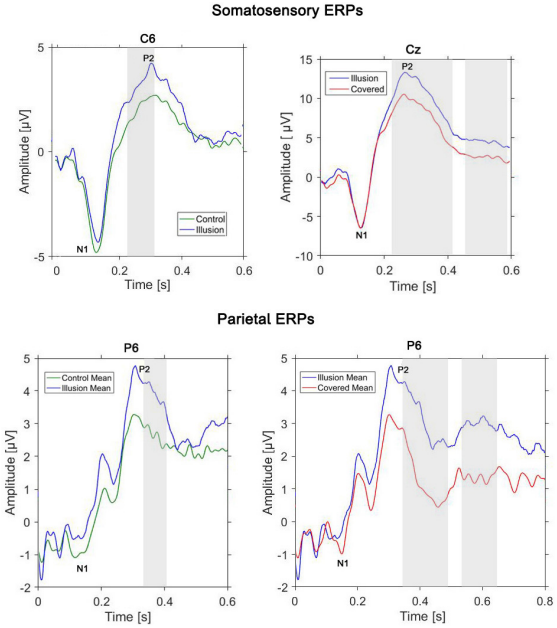

Figure 5: *High-intensity nociceptive averaged ERP waveforms between different conditions recorded on electrodes C6, Cz and P6. Control is indicated by a green color, illusion by a blue and covered by red. N-wave and P-wave indicate the negative and the positive peaks respectively and the shading area shows the time window where there is significant difference between the conditions.*

Subjective pain ratings

The analysis of the subjective pain ratings did not show any significant effect among the three conditions. Previous studies have shown an analgesic effect of viewing the body part on intensity of pain [10, 12, 16], therefore the opposite effect was expected during the illusion and covered condition since the participants could not see their hand. However, there is not enough evidence to support previous results. Nevertheless, the results of the present study are relevant with the ones of Torta et al. 2015 where they did not observe any significant effect in the perception of pain [15]. Moreover, Thøgersen et al. 2017 also found no significant differences on heat and cold thermal thresholds between illusion and control conditions with the use of the same illusory method as in the present study [19].

In the present experimental procedure, two different intensities were used for the electrical stimulation, in order to avoid habituation and/or sensitization and to observe different effects on pain perception. A possible reason for not having significant differences among the conditions on pain ratings might be the fact that the participants were not familiarized with the VAS before the trial. A possible suggestion could be recruiting people with a previous experience in pain experiments so that they are used to the VAS or train the participants before the experiment so that they will be more familiarized with the way VAS works.

Proprioceptive drift

The illusion caused a proprioceptive drift in the most distant measured points from the participants' view, more specifically the tip of the index finger and the knuckle. The drift indicated that the loss of visual feedback can affect proprioception and body-awareness. These results replicate the findings of Thøgersen et al. where it was shown that this illusory method can change the body representation in healthy participants [19]. Furthermore, a significant difference was found for the location of stimulus between control and illusion conditions. This shows that the lack of visual feedback of the limb can not only influence the body perception but also the perceived location of the stimuli. This finding may indicate that in post-amputation patients phantom pain arising in the stump can be the combined effect of the lack of visual feedback and the effect the deafferentation.

Event-related potentials

In contrast to the pain ratings, the loss of visual feedback had a significant effect on the ERPs. There was an increase in the amplitude of P2-wave during illusion which shows that, when the participants' limb disappeared, their cortical responses were larger compared to both control and covered conditions. These results are in line with several studies that have induced cortical changes by illusory methods [8, 11, 19, 23, 24]. This finding is also compatible with previous findings where it has been shown that the amplitude of laser-evoked potentials (LEPs) was smaller when the participants were looking at their own hand [12]. On the contrary, this effect was not observed during the covered condition where the cortical responses were significantly different from the control condition. Furthermore, the peak latencies of N1-wave in control condition were significantly different compared to illusion and covered. Particularly, N1-wave appeared earlier during control condition. The latency of the N1 component of a visual event related potential has been suggested to reflect the time taken for an individual to distinguish visually-attended stimuli [25, 26]. Therefore, the later responses, when the visual feedback of the limb is absent, may indicate that greater processing effort is needed.
Significant differences between control and illusion conditions were found in the parietal cortex. The parietal cortex is responsible for integrating sensory and proprioceptive inputs and is suggested to be involved in egocentric spatial awareness and visual covert attention [27]. Therefore, the enhanced responses during illusion condition may reflect more abstract mental representations instead of pure sensory processing [27]. The enhanced activation in the brain along with no significant differences in the subjective pain ratings may suggest that these amplified responses are not caused because of the change in pain perception but probably due to a visuo-spatial mismatch.

The purpose of applying electrical stimulation with the CPE electrode was to activate nociceptive Aδ fibers in order to investigate pain perception. From the results it seems that the stimulation was not entirely nociceptive specific. Particularly, the ERPs presented early components $\sim$ 50 ms, showing faster conduction velocities which are related to the activation of non-nociceptive fibers. Another characteristic of activation of nociceptive fibers is the sharp P-wave, which was not present in the majority of ERPs [28, 29, 30, 31].

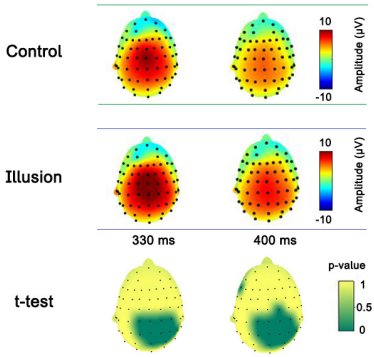

Figure 6: *Topographies of the ERPs between control and illusion conditions at different time points, 330 ms and 400 ms, for each t-test with the significance showed in the last row. The different time points were selected based on the significance range.*

Even though the applied electrical stimulation was not nociceptive specific, the ERPs largely reflect the processing of salient stimuli and the reorientation of attention. This can also be seen in the incongruence between the cortical responses and the subjective pain ratings. Iannetti et al. 2008 have shown that the laser-evoked

responses are an ambiguous output of the central nociceptive processing, although these processes can be triggered by any salient stimulus regardless the sensory modality [29].

The amplitude of ERPs was not significantly different between control and covered conditions. However, the mean values for the amplitude of P2-wave showed a reduction of cortical activity during the covered condition compared to control. This finding stays in contrast with the hypothesis that not seeing the limb increases the cortical responses. It is possible, however, that the setup of the present experiment may have influenced the results for the covered condition. A soft towel was used to cover the participants' left limb, which created a touch sensation during the electrical stimulation. According to the gate-control theory of pain by Melzack and Wall, the activation of large myelinated tactile fibres affects and may inhibit the transmission of signals from nociceptors to the brain [32]. During covered condition, it is possible that the tactile feedback from the towel caused an inhibitory effect on the activation of nociceptors. However, the arrival of the tactile signal was not time locked and the signal was continuous, thus not controllable by the experimenters. Nonetheless, even when the arrival of the two stimulations to spinal cord is not synchronized there still can be an inhibitory effect [33]. Nevertheless, it cannot be stated that the effect on the ERPs in covered condition is a definite result of the inhibitory mechanism because the tactile feedback was not controllable.

V. Conclusion

This study shows that the phantom limb illusion temporarily affected cortical responses and body awareness. The current findings may indicate that loss of the visual feedback by itself can modulate somatosensory processing. Moreover, the MR system created a realistic and immersive illusion for the participants. This can be further investigated in research between PLP patients and healthy participants. With the use of this system healthy participants can experience a phantom illusion. This will allow to investigate whether there is a difference in cortical responses between the two groups. Additionally, future research is needed to test if the effect on cortical responses and proprioception caused by the phantom limb illusion can be permanent.

References

[1] M. Hanley, M. Jensen, D. Smith, D. Ehde, W. Edwards, and L. Robinson, "Preamputation pain and acute pain predict chronic pain after lower extremity amputation," *The Journal of Pain*, 2007.

[2] S. Griffin and J. Tsao, "A mechanism-based classification of phantom limb pain," *Pain*, 2014.

[3] M. Sumitani, S. Miyauchi, A. Yozu, Y. Otake, Y. Saitoh, and Y. Yamada, "Phantom limb pain in the primary motor cortex: topical review," *Journal of Anesthesia*, 2010.

[4] B. Subedi and G. T. Grossberg, "Phantom limb pain: Mechanisms and treatment approaches," *Pain Research and Treatment*, 2011.

[5] H. Flor, L. Nikolajsen, and T. Jensen, "Phantom limb pain: a case of maladaptive cns plasticity?," *Neuroscience*, 2006.

[6] S. Das, Y. Yuan, and H. Yang, "Neuroimaging: A key unlocking phantom limb pain," *Austin Neurology & Neurosciences*, 2016.

[7] Y. Oouchida and S. Izumi, "Imitation movement reduces the phantom limb pain caused by the abnormality of body schema," *International Conference on Complex Medical Engineering*, 2012.

[8] M. Sumitani, S. Miyauchi, C. McCabe, M. Shibata, L. Maeda, Y. Saitoh, T. Tashiro, and T. Mashimo, "Mirror visual feedback alleviates deafferentation pain, depending on qualitative aspects of the pain: a preliminary report," *Rheumatology (Oxford)*, 2008.

[9] M. Diers, W. Zieglgansberger, J. Trojan, A. Drevensek, G. Erhardt-Raum, and H. Flor, "Site-specific visual feedback reduces pain perception," *PAIN*, 2013.

[10] B. Chan, R. Witt, A. Charrow, A. Magee, R. Howard, P. Pasquina, K. Heilman, and J. Tsao, "Mirror therapy for phantom limb pain.," *The New England journal of medicine*, 2007.

[11] S. Kim and Y. Kim, "Mirror therapy for phantom limb pain," *Korean Journal of Pain*, 2012.

[12] M. Longo, V. Betti, S. Aglioti, and P. Haggard, "Visually induced analgesia: Seeing the body reduces pain," *Journal of Neuroscience*, 2009.

[13] J. Hunter, J. Katz, and K. Davis, "The effect of tactile and visual sensory inputs on phantom limb awareness," *Brain*, 2003.

[14] M. Botvinick and J. Cohen, "Rubber hands 'feel' touch that eyes see," *Nature*, 1998.

[15] D. Torta, V. Legrain, and A. Mouraux, "Looking at the hand modulates the brain responses to nociceptive and non-nociceptive somatosensory stimuli but does not necessarily modulate their perception," *Psychophysiology*, 2015.

[16] R. Matthew, G. Iannetti, F. Mancini, J. Driver, and P. Haggard, "Linking pain and the body: Neural correlates of visually induced analgesia," *The Journal of Neuroscience*, 2012.

[17] D. Lelic, C. Mø rch, K. Hennings, O. Andersen, and A. Drewes, "Differences in perception and brain activation following stimulation by large versus small area cutaneous surface electrodes," *European Journal of Pain*, 2011.

[18] M. Churyukanov, L. Plaghki, V. Legrain, and A. Mouraux, "Thermal detection thresholds of adelta- and c-fibre afferents activated by brief co2 laser pulses applied onto the human hairy skin," *PLoS One*, 2012.

[19] M. Thø gersen, J. Hansen, L. Arendt-Nielsen, H. Flor, and L. Petrini, "A visual feedback system using mixed reality to simulate a phantom limb illusion in healthy volunteers," *Unpublished manuscript*, 2017.

[20] H. van Stralen, M. van Zandvoort, S. Hoppenbrouwers, M. Vissersa, L. Kappelle, and L. Dijkerman, "Affective touch modulates the rubber hand illusion," *Cognition*, 2013.

[21] M. Rohde, M. Di Luca, and M. Ernst, "The rubber hand illusion: Feeling of ownership and proprioceptive drift do not go hand in hand," *PLoS One*, 2011.

[22] A. Delorme and S. Makeig, "Eeglab: an open source toolbox for analysis of single-trial eeg dynamics including independent component analysis," *Journal of Neuroscience Methods*, 2004.

[23] M. Schaefer, H. Flor, H. Heinze, and M. Rottea, "Morphing the body: Illusory feeling of an elongated arm affects somatosensory homunculus," *NeuroImage*, 2007.

[24] M. Longo, S. Pernigo, and P. Haggard, "Vision of the body modulates processing in primary somatosensory cortex," *Neuroscience Letters*, 2011.

[25] A. Latham, L. Patston, C. Westermann, I. Kirk, and L. Tippett, "Earlier visual n1 latencies in expert video-game players: A temporal basis of enhanced visuospatial performance?," *PLoS One*, 2013.

[26] E. Callaway and R. Halliday, "The effect of attentional effort on visual evoked potential n1 latency," *Psychiatry Research*, 1982.

[27] A. Schindler and A. Bartels, "Parietal cortex codes for egocentric space beyond the field of view," *Current Biology*, 2012.

[28] G. Iannetti, "The electrocortical responses to nociceptive stimulation in humans," *Pain*, 2010.

[29] G. Iannetti, N. Hughes, M. Lee, and A. Mouraux, "Determinants of laser-evoked eeg responses: Pain perception or stimulus saliency?," *Journal of Neurophysiology*, 2008.

[30] I. Ronga, E. Valentini, A. Mouraux, and G. Iannetti, "Novelty is not enough: laser-evoked potentials are determined by stimulus saliency, not absolute novelty," *Journal of Neurophysiology*, 2013.

[31] A. Mouraux, G. Iannetti, and L. Plaghki, "Low intensity intra-epidermal electrical stimulation can activate adelta-nociceptors selectively," *PAIN*, 2010.

[32] R. Melzack and P. Wall, "Pain mechanisms: A new theory," *Science*, 1965.

[33] K. Inui, T. Tsuji, and R. Kakigi, "Temporal analysis of cortical mechanisms for pain relief by tactile stimuli in humans," *Cerebral Cortex*, 2005.

Table of Contents

Table of Contents

Background 1

Phantom pain was firstly described by Ambrose Pare, a 16th French military surgeon, as a kind of perceived pain in a body region that no longer exists. In the 19th century, Silas Weir Mitchell, a civil war surgeon, coined the term "phantom limb pain" (PLP) [1]. PLP is a type of neuropathic chronic pain which occurs up to 85% of patients who have undergone amputation surgery. The onset of PLP can be immediate, but it can also appear for the first time many years after amputation [2]. Besides pain most amputees additionally perceive non-painful sensations which are related to the feeling that the missing limb is still present. Thus, when applying touch or pressure to the residual limb, the amputees often feel the same modality of sensation on the phantom limb [1]. The phantom phenomena (painful and non-painful sensations) seem to be more drastic in the distal parts of the phantom and have been described in various ways such as stabbing, throbbing, burning or cramping. Numerous researchers have tried to investigate the mechanisms behind phantom sensations and phantom pain [1, 3–9]. However, it still remains a poorly understood medical condition and thus, difficult to treat [1].

1.1 PLP Mechanisms

The pathophysiology and etiology of phantom limb pain have been extensively investigated. Both central and peripheral mechanisms have been posited and some researchers propose that PLP is derived from both of them [1, 5].

1.1.1 Peripheral Nervous System Mechanisms

The peripheral nerves are damaged after amputation. This damage affects the normal way that afferent nerve input is transmitted into the spinal cord. Subsequently, this causes the creation of neuromas. In these neuromas, there is an excessive expression of sodium channels because of an advanced accumulation of signaling molecules (i.e neurotransmitters, kinins and other peptides, neurotrophic factors etc.) and this results to hyperexcitability and impulsive discharges. This irregular peripheral activity can contribute to phantom phenomena [1, 4].

1.1.2 Central Nervous System Mechanisms

Cortical reorganization is the most cited central nervous system (CNS) mechanism for PLP [1, 5–9]. Following amputation, changes have been found in brain regions such as the primary somatosensory (SI) and the motor cortex (MI). These brain regions are shown in figure 1.1. The area that represented the amputated part is shrunk whereas the representations of the adjacent areas are expanded. Moreover, it was proved by fMRI studies that the magnitude of SI reorganization is positively correlated to the intensity of PLP [1, 2, 5].
Another suggested central mechanism is the alteration of the body schema, which was firstly proposed by Head and Holmes in 1912 [10]. The body schema is described as a constantly altering spatial template of the human body inside the brain and it is updated during body movements [11]. It integrates different sensorimotor inputs such as tactile, visual, proprioceptive and efferent commands. The continuous update of all these inputs, makes the body schema adaptable and plastic to any change in the body surface [11]. A similar, but more extensive and widespread theory was introduced in Ronald Melzack's "Neuromatrix" theory [9]. Neuromatrix is a network of neurons within the brain that combines information from the body such as somatosensory, limbic, visual and thalamocortical and results in perceptions of pain and/or other essential sensations. The neuromatrix engages the sensory, affective and cognitive aspect of the experience of pain and also it maintains a central representation of the limbs which can be modified by new experiences. [1, 5, 9]

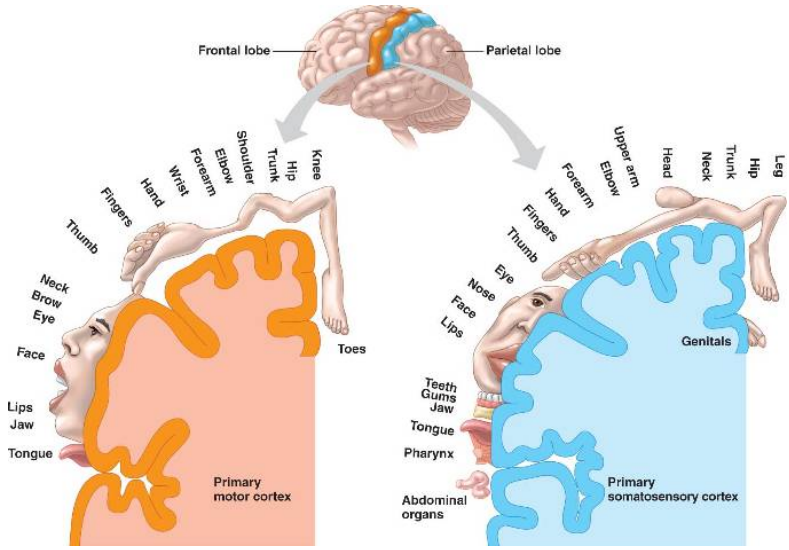

Figure 1.1: *Graphical representation of the primary Somatosensory(SI) and Motor(MI) cortex and the somatotopic map of the body within the brain.*

1.2 Residual limb phenomena

Pain in the residual part of the amputated limb or non-painful sensations have also been noticed as a consequence of amputation and they are perceived on the body part that still exists and it is close to the deafferentated area [2]. Telescoping is another experience after amputation which refers to a phenomenon where the phantom moves closer to the location of the amputation [2, 12]. Previous research has shown that telescoped phantoms trigger areas remote from the cortical area that represented the amputated limb whereas non-telescoped phantoms convey sensory and motor feedback to the area representing the amputated limb [12]. Furthermore, there are studies on illusory and imagery perceptions in PLP patients that showed that SI responds to the perceived and not the actual feedback from the respective sensory system [2, 13–15].
These data indicate that there is correlation between cortical reorganization after amputation and residual limb phenomena and also support the approach that visual, sensorrimotor feedback and spatial-awareness play a crucial role for phantom limb phenomena in general [2].

1.3 Modulation of pain perception by visual illusions

The multiple feedbacks and their correlation with phantom limb phenomena have been broadly studied by many researchers, especially how the visual feedback modulates pain perception and body-awareness [16–21]. Mancini et al 2011 showed that viewing a distorted image of the body regulates pain perception, where the enlarged body image induced analgesia and the shortened image decreased it [18]. Mirror box illusion is one of the methods used in these studies and it is shown in figure 1.3. During mirror box illusion participants view the reflection of their intact body part in the position of the amputated part [19]. Several studies have shown that this method may temporally relieve phantom limb pain [19–21]. Furthermore, another method that has been used is the rubber hand illusion shown in figure 1.3 which combines visual illusion and body-ownership awareness. During this method the therapist or the experimenter strokes a participant's hand hidden from their view and simultaneously strokes a visible rubber hand. The illusion can be quite realistic that people feel the rubber hand as if it was their own hand [22, 23].

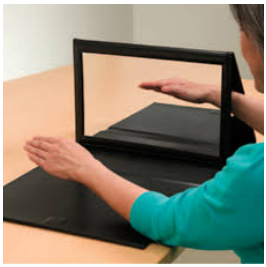

Figure 1.2: *Mirror box illusion*

Figure 1.3: *Rubber hand illusion*

Along with the pain perception, researchers have also investigated brain activity by electrophysiological and imaging methods [16, 17, 24, 25]. The electrophysiological studies have used electroencephalography (EEG) to investigate the event related potentials (ERPs) during nociceptive and/or non-nociceptive stimulation. It was shown that visual analgesia reduced the magnitude of ERPs [17]. Moreover, the ERPs of a PLP patient group were larger than those from a healthy group [25]. Additionally, fMRI studies have revealed an association between cortical reorganization and PLP [16, 25]. Taken together, it seems that the perception and processing of pain is strongly affected by the ability to see the body that is perceived as one's own. Particularly, previous findings suggest that pain sensitivity is increased when the visual feedback is absent.

Aim 2

Numerous studies have investigated PLP mechanisms with illusory methods. However, the illusions were created mainly by adding something additional to the participants' vision, thus tricking the brain. In the present study the effect of loss of visual feedback on pain perception was investigated by applying a new approach. With the use of a novel mixed reality system, which enables a more realistic and engaging experience, the participants encountered a phantom limb illusion where their left hand and forearm disappeared from their view. The aim of the study is to investigate the responses to nociceptive electrical stimulation during this illusion by analyzing behavioral and electrophysiological data. Behavioral data, such as pain intensity ratings and proprioceptive drift, were used to investigate perception and localization of pain respectively, whereas electroencephalography (EEG) was used to analyze cortical responses. It was hypothesized that during the phantom limb illusion the subjective pain ratings and cortical activity were increased and there was a mismatch in proprioception.

Materials & Methods 3

3.1 Electroencephalography

Electroencephalography (EEG) is a neuroimaging method that has been used in numerous studies in order to record electrical signals also known as brain waves. It is commonly used in medical and research areas. The recording of cortical activity is done by metal electrodes placed on the scalp. A standard electrode placement is commonly used in EEG measures, known as the 10-20 system. The head is divided into particular regions (nasion, preauricular points, inion) and they are located in proportional distances. The electrodes are placed in these proportional distances and represent particular brain regions. The 10-20 label refers to the distance in percents between the nose and ears for each electrode as it is shown in figure 3.1 [26].

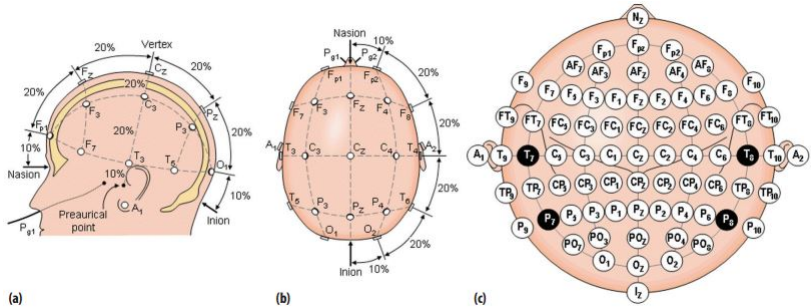

Figure 3.1: *The 10-20 electrode placement system [26].*

3.1.1 Event-related potentials (ERPs)

EEG records neural activity which is related to both sensory and cognitive processes and has a high temporal resolution. Therefore, it is a useful method to investigate time locked events, i.e. ERPs. ERPs represent brain activity in small voltages and they are caused by specific events or stimuli. They can be elicited by many sensory, motor and cognitive stimuli and they can be divided in two phases. The early phase called 'sensory' or 'exogenous' waves are elicited within the first 100 ms after the onset of stimulus and they are highly related to the physical parameters of the stimulus. The later phase is called 'cognitive' or 'endogenous' and it represents the way a person perceives the stimulus hence it is related to information processing [27].
The waveform of ERP consists of a series of positive and negative peaks known as ERP components and they are characterized by their amplitude and latency as shown in figure 3.2. The ERP components represent the primarily cortical activity with a small contribution of subcortical structures and can be used as markers of cognitive processes. Changes in the cognitive processing can be reflected in the particular components of an ERP. This can be useful while investigating if any change in the mental state affects sensory and cognitive processing. Specifically, changes in the amplitude of a component indicate a change in the input of the process or a change in the process itself and changes in the peak latency of the component indicate that the duration of the process is affected [28].

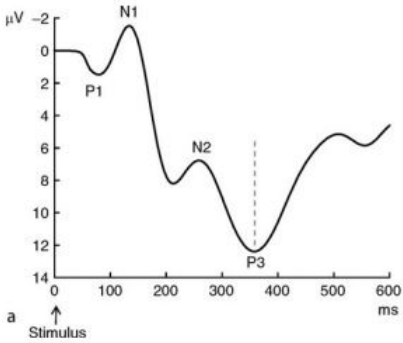

Figure 3.2: *Illustration of ERP components. The N represents the negative wave and the P represents the positive wave [28].*

Several components have been well investigated in relation to different stimulation modalities. Particularly early components P1 and N1 are known to reflect the activation of modality-specific areas such as visual and auditory cortex [27, 28]. The N1 component also occurs in response to heat [29], pain [29] and somatosensory stimuli [30]. The N1 component has its peak between 90 and 200 ms and it is activated when unexpected stimulus is applied [27]. Its activation is mostly distributed across fronto-central brain areas. The amplitude of P1 component is related to the attention on the stimulus [28]. Late components are related to central cognitive processes. P2 which peaks at around 100-250 ms is correlated with various higher-order cognitive processes. The N1/P2 components together are supposed to demonstrate the sensation-seeking behaviour [27, 28]. Another known endogenous component is the P3 component, which peaks between 250-400 ms [27]. It is thought to resemble

the update of the contextual memory or transitory filtering of the stimulus which is significant for motivation. The latency of this component is suggested to indicate the end of the processes, which evaluate the stimulus [28]. The morphology of ERPs differs as a function of sensory modality. Particularly cortical responses to different stimuli reflect different modalities [31]. Mouraux et al. 2008 have shown a classification of different modalities and the respective ERPs which can be seen in figure 3.3 [32]. It can be noticed that somatosensory ERPs (nociceptive and non-nociceptive) have positive peaks amplified compared to the rest of ERPs. For nociceptive and auditory the N peak is the most amplified. The visual ERPs has the lowest amplitude in the positive peak and it is also the least sharp waveform. In the non-nociceptive somatosensory ERPs early responses can be noticed. The latencies of the auditory and non-nociceptive somatosensory ERPs are similar for both negative and positive peaks (N around 100 ms and P between 200 and 300 ms). The visual ERP peaks slightly later, its negative peak is at around 150 ms and positive is after 300 ms. The latest response to the stimuli can be seen in the nociceptive ERP where the negative peak is at 200 ms and positive at around 350 ms. This late response is related to the morphology of the nociceptive fibers which have smaller diameter than the others, hence the transmission of the signal to the cortex is slower.
ERPs construct a millisecond-by-millisecond evidence of neural activities associated with sensory encoding, inhibitory responses and updating working memory. It allows for a noninvasive investigation of brain function so it is useful for cases as phantom limb pain which includes not only sensory processes but also cognitive ones [27, 33].

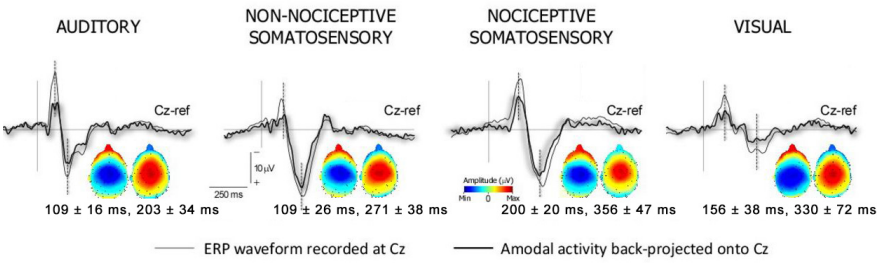

Figure 3.3: *Different sensory modalities and respective ERPs [32].*

3.1.2 EEG data processing

Before obtaining the ERPs, EEG raw data require pre-processing. Some of the most important steps of the preprocessing procedure are the filtering, epoch segmentation and independent component analysis (ICA).

3.1.2.1 Filtering

In general, the digital filters are divided into two categories: the infinite impulse response (IIR) and the finite (FIR). IIR filters meet the requirement of low filter order which makes them fast in execution. However, they are not easy to control because they do not have a linear phase response [34]. Whereas FIR filters make a linear phase possible and they are always stable but require more memory. The output of the FIR filters is a weighted sum of the most recent input values as it shown in equation3.1:

$$y(n) = b_0 * x(n) + b_1 * x(n-1) + \cdots + b_N * x(n-N) = \sum_{i=0}^{N} b_i * x(n-i) \tag{3.1}$$

where x(n) is the input signal, y(n) is the output signal, N is the filter order b_i is the value of the impulse response at the i'th instant for $0 \leq i \leq N$ of an Nth-order FIR filter
In order to remove noise from the EEG data both a FIR high pass and low pass filters were used. The low pass filter was set at 0.5 Hz and the high pass at 40 Hz. The filtering was applied in the continuous data to avoid unwanted artifacts at the epoch boundaries.

3.1.2.2 Epoch Segmentation

EEG signal is non-stationary which means that the statistical features (means and variances) of the signal change over time. At any given sample, the EEG signal of an electrode, reflecting the brain activity and its source, is in a continuous change. Due to this, the sampling data is also in a continuous change, so processing EEG with its whole length may not yield optimal results. Therefore, the signal was split to smaller segments, called epochs. The EEG signal of a single epoch is assumed to be stationary [35]. For further analysis of the signal, epochs of 2 s were chosen, time locked on the time of the stimulation allowing for ERP detection.

3.1.2.3 Independent Component Analysis

Each data epoch represents a trial, time locked to the moment of stimulation. In the preprocessing, the detection and rejection of artefacts that contaminate the event-related EEG data are critical. An efficient method for this is the independent component analysis (ICA). Before ICA, the data epochs may contain temporal muscle artifacts, eye blinks or eye movements. These artefacts usually have higher amplitudes relative to brain signals and even if they are not happening regularly they can bias the averaged evoked potentials or other measures computed from the data [36]. ICA separates artefact sources, whose effects on the signal are maximally independent of one another, but requires a lot of data. In more details, ICA finds a coordinate frame where the recorded signals can be projected into the independent component space. A linear change of coordinates from the electrode space to the independent component space is represented by the multiplication of the scalp data X by the weighted matrix W found by ICA algorithm and is shown in equation 3.2

$$S = W * X \tag{3.2}$$

where S is the activation matrix of the components over time. Each component is a linear weighted sum of the activity of the independent source projecting to all the electrodes. The rows of the W matrix that constitute each component activity time course can act as spatial filters for a different activity pattern in the data. Every component contains an activation time course and a scalp map which is the corresponding column of the W matrix (W^{-1}). The scalp map reveals the relative projections strengths and polarities of the component to each of the electrodes and an example is shown in figure 3.4 [36].

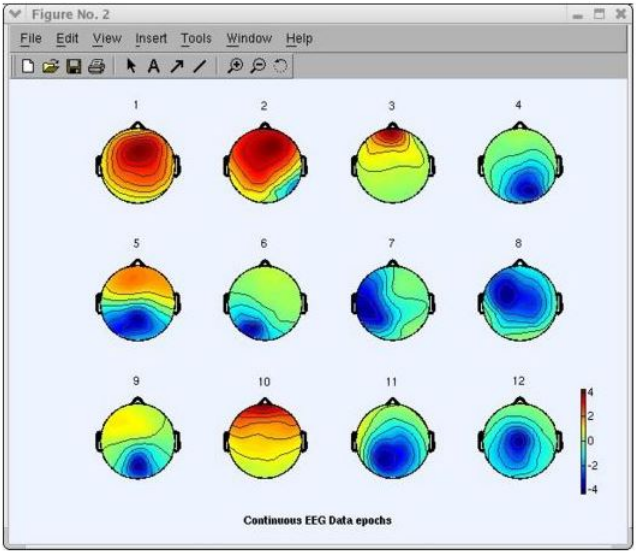

Figure 3.4: *An example of scalp map projection of selected components. The scale of the components' activity is in arbitrary units [37].*

An automated version of ICA algorithm was used in the preprocessing procedure, called *runica()* and it is implemented in EEGLab software toolbox. This version is preferable when strong electrical artifacts are present in the data and it gives a stable decomposition. Runica algorithm detects only high peak activity. Therefore, an option was set as "'extended', 1" so that it can also detect line current and/or slow activity [37].

3.2 Visual Analog Scale

Visual Analog Scale (VAS) is a measure to assess pain intensity. It is a continuous scale consisting of a 10 cm line and it is widely used in experiments with pain. For pain intensity the scale is most commonly fixed in a way that 0 means no pain, 5 is moderate pain and 10 is unbearable pain as it is shown in figure 3.5. It can be used both by a ruler which the subject moves up and down on the scale and verbally when the subjects says a number from 0 to 10 in order to describe how intense the perceived pain is which is called numerical rating scale (NRS) [38]. It this study it was used as a verbal scale, after each stimulation.

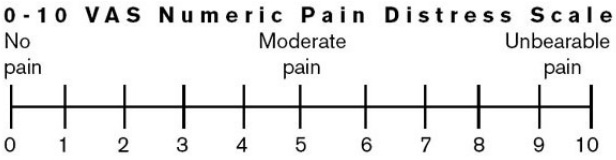

Figure 3.5: *Example of A Visual Analog Scale.*

3.3 Proprioceptive drift measurement

The proprioceptive drift is a measurement which has been used in studies related to the rubber hand illusion [12, 22, 39]. It is used as an indicator of how a person perceives the spatial layout of their body. The method is usually used on a horizontal or vertical position across the subject and spots the proprioceptive drift in relation with another object [12] . In this study, the proprioceptive drift was measured through a slider on a ruller which was positioned underneath a table and participants were using their right hand (contralateral of the stimulation) to localize different anatomical parts of their left arm as it is shown in figure 3.6. These anatomical parts are the tip of the index finger, the knuckle and the wrist. Additionally, they were asked to report the perceived location of stimulus.

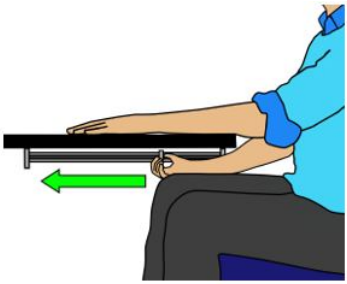

Figure 3.6: *A display of the proprioceptive drift measurement [12].*

3.4 Mixed Reality System

Mixed reality (MR), is the combination of real and virtual worlds in order to create new environments and visualizations where real and digital objects co-exist and interact in real time. When it comes to human-computer interaction, the integration of the physical and digital aspects has to occur in a mild and adaptable way. There are several examples of MR usage such as augmented reality, embodied interfaces, augmented virtuality and concrete user interfaces [40] [41]. A term that has been often used to represent the link among augmented reality, virtual reality and stages in between is the virtual continuum by Milgram and Kishino shown in figure 3.7 [40]. The name "Mixed Reality" is used as a unified name for all the stages. MR systems have been used in various fields such as medicine, military and industrial applications, entertainment and games and distance or remote support and also

geographic applications. In medicine there are studies that have used a Virtual reality-based system for multisensory feedback training [33, 42] to induce visual analgesia.

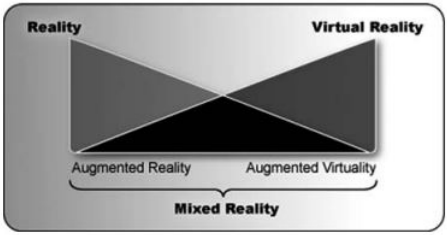

Figure 3.7: *The virtual continuum by Milgram and Kishino. [40]*

The present study used a novel MR system to interfere with the participants' visual feedback. Particularly, by creating an illusion where their hand and forearm disappeared. This was done by merging a green-screen technology with MR technology. The green-screen technology is a graphical technique in which the green color becomes transparent or removed and then replaced by a desirable background picture [43]. In this study the picture of the background (a table covered with black material) was taken and a green glove was placed on the participants hand. Then, the green glove was replaced by the blackground color making the hand disappear from the participants' view [12]. The design of MR system was created by Thøgersen et al. 2017 and included the use of an Oculus Rift® (Developer kit 2, Oculus VR, LLC, USA) shown in figure 3.8 with two 60 fps SXGA cameras (uEye® UI-3241LE-C-HQ, Imaging Development Systems GmbH, Germany), which were fixed to the Oculus in the position directly in front of the participants' eyes. The advantage of this system is that the camera streams directly to the screens of the oculus rift, allowing to modify the video streams in real-time to create an illusion [12]. The illusion was created by a fading method implemented in Unity software(Copyright © 2017 Unity Technologies).

Figure 3.8: *Oculus Rift mixed reality system.*

3.5 Electrical stimulation

There are several fibers that are responsible for transferring the somatosensory stimulus. They are called primary afferents and can be classified depending on various criteria (figure 3.9). They vary in axonal diameter, which is related to the conduction velocity, in the peripheral targets and in the type of the stimulus to which they are responding to. They also vary in terms of myelination. Very small and unmyelinated afferents are called C-fibers, whereas myelinated fibers can be divided into the large-diameter - Aβ fibers and the small-diameter -Aδ fibers. From these groups, the C-fibers and Aδ fibers carry nociceptive activations from the nociceptors, while Aβ fibers are low-threshold mechanoreceptors related to the touch and hair movement.

Receptor Type	Modality	Axonal Diameter[a]	Conduction Velocity[a]
Aβ Fiber Group			
Low-threshold mechanoreceptors	Discriminative touch	10 µm	60 ms−1
Aδ Fiber Group			
Nociceptors	Pain	2.5 µm	12 ms−1
Cool receptors	Temperature	–	–
C Fiber Group			
Nociceptors	Pain	1 µm	<2 ms−1
Warm and cool receptors	Temperature	1 µm	<2 ms−1
Itch receptors	Itch	1 µm	<1 ms−1
Low-threshold mechanoreceptors (CT)	Emotional Touch	1 µm	<2 ms−1

Figure 3.9: *Main properties of primary afferents. Taken from lecture slides of Sensory Systems and Sensory-Motor Control (Author: Shellie A. Boudreau, Associate Professor).*

The activation of Aδ fibers is related to fast pain and the activation of C-fibers is related to slow pain [44]. Fast pain is also known as first pain because it is the first response to nociceptive stimuli. Additionally it creates a well localized pricking sensation compared to slow pain. In contrast, slow pain is called second pain, which occurs after some time and gives burning and aching sensation. The illustration of fast and slow pain is shown in figure 3.10

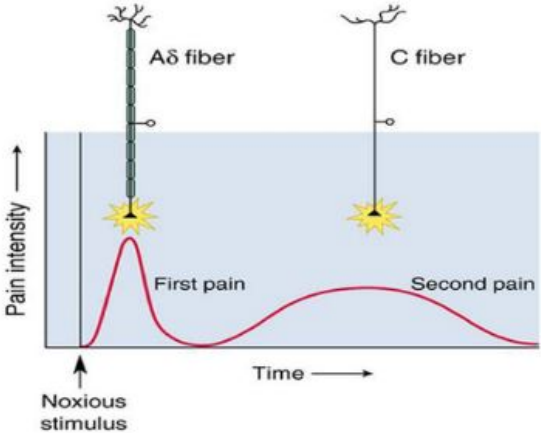

Figure 3.10: *The response of Aδ and C fibers to nociceptive stimulus. Taken from lecture slides of Sensory Systems and Sensory-Motor Control (Author: Shellie A. Boudreau, Associate Professor).*

In order to study pain there is a need to experimentally apply stimulus which activates nociceptive fibers. There are several methods to provide nociceptive stimulation such as contact heat, mechanical pin prick, laser heat and electrical stimulation [45]. Each of the methods aims to create ideal painful stimulation, but each of them has also its drawbacks. Ideally, the method should provide a stimulation that is nociceptive, which means that it should elicit potentials only on the fibers that are responsible for conducting nociceptive information, it should also be safe, controllable and reproducible [46]. One of the methods which meets the above mentioned criteria and is the most used in clinical and experimental environments is the laser method, which uses a laser beam to deliver pain. The biggest advantage of this method is the fact that the laser beam does not contact the skin directly, which results in selective activation of only nociceptors without concomitant activation of mechanoreceptors and Aβ fibers [45, 46]. However, if high-intensity stimulation is used the laser beam could burn the superficial skin making the method unpleasant for the participants [46]. Another limitation is the fact that stimuli have to be separated by long lasting intervals (between 5-20 s) to avoid sensitization or habituation. Long time is needed for conduction of the nociceptive signal, which results in a non ideal synchronization of the arrival of the signal [47]. Moreover laser stimulators are big and expensive devices, which is not desired in clinical settings [48].
Another widely used method for nociceptive activation is electrical stimulation through surface electrodes. This method is cheap and easy to use. However, conventional surface electrodes activate not only nociceptive fibers but also non-nociceptive, because of the higher activation threshold of the first. This happens because the activation occurs by the density current which depolarizes the fiber membrane itself instead of activating receptor properties and transduction mechanisms. The first solution to solve the problem of specificity during electrical stimulation was the introduction of intra-epidermal electrodes. The intra-epidermal method was based on the fact that the endings of the nocicieptive fibers are located in epidermis. Thus by creating an electrode that reaches only the epidermal receptors selectivity can be achieved. Kaube et al. 2000 suggested that the possible cause of more selective activation of the nociceptors while using these electrodes may be the fact that they create a higher current density at the epidermal junction [49]. Moreover, while using electrodes with smaller stim-

ulation area, the nociceptors can be activated with lower-intensity than mechanoreceptors [50]. The differences between these methods can be seen in the latencies of the N-P complex. Table 3.11 shows differences in the N-P latencies between these methods, indicating the higher selectivity of laser and intra-epidermal methods [47].

	ES	LS	IES	
N latency	134 ± 13	274 ± 35	2 × threshold	199 ± 47
			0.25 mA	159 ± 39
			2.5 mA	145 ± 75
P latency	293 ± 85	399 ± 57	2 × threshold	369 ± 83
			0.25 mA	340 ± 111
			2.5 mA	312 ± 67

Figure 3.11: *Latencies of N-P complex of three different stimulation methods: ES - surface non-nociceptive electrical stimulation, LS - laser nociceptive stimulation and IES - intra-epidermal nociceptive stimulation. The latencies are given in milliseconds [47].*

To provide selective and specific activation of nociceptors by non-invasive electrodes a novel non-invasive electrical stimulation method has been introduced. A new concentric pin electrode shown in figure 3.12 was used in the present study, which can stimulate in high current density at a low current intensity [45]. This means that the depolarization activates only superficial layers of the skin, where Aδ nociceptive fibers are located, without activating deeper layers. The electrode was placed on the participants' left forearm at around 1/3 length from the wrist to the elbow on the ventral side. Additionally, the detection threshold and the stimulation intensities used for each participant during the experiment can be found in Appendix I.

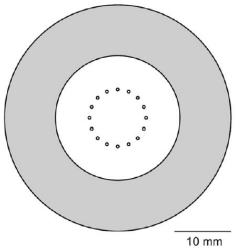

Figure 3.12: *The design of the concentric pin electrode (CPE) [50].*

3.6 Statistical Analysis

The statical tests were performed in SPSS ® 24 (IBM Inc., USA) and Matlab R2016b ® (MathWorks Inc., USA) with Letswave toolbox (http://www.nocions.org/letswave/).

3.6.1 Normality test

To test if the sample comes from a population where the members follow a normal distribution the Shapiro-Wilk method was used in SPSS for the behavioral data (proprioceptive drift and subjective pain ratings). This method is fitting better in cases with small sample sizes but it can also handle a large amount of samples. The Shapiro-Wilk test, tests the hypothesis that a sample x_1,...,x_n comes from a normally distributed population [51].The statistic W is calculated as it is shown in equation 3.3 :

$$W = \frac{\left(\sum_{i=1}^{n} a_i x_{(i)}\right)^2}{\sum_{i=1}^{n}(x_i - \bar{x})^2}, \tag{3.3}$$

where x_i is the ith order statistic, for example the ith smallest number of the sample; $\bar{x} = (x_1 + ... + x_n)/n$ and the constants a_i are given by the equation 3.4

$$(a_1, \ldots, a_n) = \frac{m^{\mathsf{T}} V^{-1}}{(m^{\mathsf{T}} V^{-1} V^{-1} m)^{1/2}}, \tag{3.4}$$

where $m = (m_1, \ldots, m_n)^{\mathsf{T}}$ $m = (m_1, \ldots, m_n)^{\mathsf{T}}$ and $m_1, \ldots, m_n m_1, \ldots, m_n$ are the expected values of the order statistics of independent and likewise distributed random variables sampled from the standard normal distribution, and V is the matrix of the covariance of those order statistics [51]. If the p-value is less than the chosen alpha level (0.05) then the hypothesis is rejected so the population is not normally distributed. The test performed to the behavioral data of the study showed that they are normally distributed.

3.6.2 Analysis of Variance

The analysis of variance (ANOVA) is a group of different statistical designs that analyze groups to find if there are differences between them and within. Depending on how many factors are to be tested the respective ANOVA test can be used [52]. For the behavioral data a one-way ANOVA with repeated measures was conducted for the proprioceptive drift (with the factor condition), a two-way ANOVA with repeated measures for the subjective pain ratings (with the factors condition and intensity) and a three-way ANOVA for the subjective pain ratings (with factors condition,intensity and gender). For the EEG data an one way ANOVA was performed with the factor condition on ERP latencies and amplitudes. ANOVA evaluates if one of the two or three factors or their interaction affects the data significantly however, it can not detect where the significance is, so post-hoc tests are needed. The concept behind ANOVA is based on calculating means and variances and the variability of factors is used to determine the F-values [52]. The basic calculations of ANOVA is the calculation of degrees of freedom, the sum of squares, and mean square as shown in the equations below:

$$DF_{\text{Total}} = DF_{\text{Error}} + DF_{\text{Conditions}} \tag{3.5}$$

where DF are the degrees of freedom.

$$SS = \sum_{i=1}^{n} (x_i - \bar{x})^2 \tag{3.6}$$

where $\bar{x}$ is the mean of all the data in the sample and SS is the sum of squares.

$$MS_{\text{Measured}} = \frac{SS}{DF_{\text{Total}}} \tag{3.7}$$

where MS is the mean of squares. After these calculations, the F value can be computed (equation 3.8) and the the p value which will determine if there is significant difference or not.

$$F = \frac{MS_{\text{Measured}}}{MS_{\text{Error}}} \tag{3.8}$$

3.6.3 Sphericity test

The ANOVA with repeated measures requires no violation of the sphericity assumption. Sphericity means that the variances of the differences between all combinations of the groups are equal. It can be connected to the homogenity of variances. For this, the Mauchly's Test of Sphericity was conducted on the data. It tests the null hypothesis that the variances of the differences are equal and if it is statistically significant ($p < 0.05$) then the null hypothesis can be rejected. In case of no violation the F-values can be used to define significance. Otherwise, the F- statistic is probably biased so corrections must be applied to the degrees of freedom (df). The df before corrections are calculated as shown in equations 3.9, 3.10.

$$df_{factor1|factor2} = (k-1), \tag{3.9}$$

$$df_{error} = (k-1) * (n-1) \tag{3.10}$$

where k is the number of repeated measures and n is the number of subjects. The three corrections that are applied on the df are: the lower-bound estimate, Greenhouse-Geisser and the Huynh-Feldt correction. All of them multiply the df by their estimated epsilon ε as shown in equations 3.11, 3.12 . When ε equals with 1 then the sphericity condition is met and the more it decreases below 1, the greater the violation of sphericity.

$$df_{factor1|factor2} = \hat{\varepsilon} * (k-1), \tag{3.11}$$

$$df_{error} = \hat{\varepsilon}(k-1) * (n-1) \tag{3.12}$$

3.6.4 Comparison between two datasets with t-test

T-test is used to compare whether the average difference between two groups is actually significant or because of random chance. The hypothesis of this test is that the two means are equal and this would mean that there is no difference in the data between the two compared conditions [52]. The calculation of the t-value is done by the equation 3.13

$$t = \frac{\bar{x}_1 - \bar{x}_2}{\sqrt{\frac{2\sigma_p^2}{n}}} \tag{3.13}$$

where x_1 and x_2 are the means of the two compared groups, σ_p^2 is the pooled variance and is used to define the standard deviation (σ^2) and n is the number of samples [52]. If the p value from the t-test is above the alpha level the hypothesis is rejected. T-test was used to compare pairs of conditions

(control vs illusion, control vs covered and illusion vs covered) in order to detect where these pairs are significantly different. The alpha level was set at 0.05.

3.6.5 Cluster-based permutation test

EEG data has a spatiotemporal characteristic because the signal is sampled at multiple sensors and multiple time points. Therefore, in EEG studies one has to deal with the multiple comparisons problem (MCP). The effect of interest is tested in a large number of pairs usually in the order of several thousands. Thus, a large amount of statistical comparisons has to be conducted but this makes it impossible to control the family-wise error rate (FWER) by standard statistical procedures. The FWER is the probability, under the assumption that there is no effect, of falsely concluding that there is a difference between the experimental conditions at one or more pairs. Thoroughly, the bigger the number of time samples, the more this probability of observing one or more significant p-values approaches one. A solution of the MCP requires a method that controls the FWER at some low, critical alpha-level (typically, 0.05 or 0.01) [53]. In this study, a cluster-based permutation test was conducted within the paired t-test. Cluster-based permutation test is built on the clustering of neighboring time-samples that all show a similar difference. In details, for two datasets, the test compares the signal on different kind of trials (depending on the experimental procedure) by means of a t-value. Then, it chooses the t-values that have absolute values above a specific threshold, clusters them based on temporal adjacency and then calculates cluster-level statistics by taking the sum of the t-values inside a cluster. Finally, it selects the largest in absolute value cluster-level statistic [53]. The above mentioned threshold was set by default on the 95th percentile of the cluster distribution which is used as a critical value at alpha-level 0.05 [24, 53].

3.6.6 Post-hoc testing

As mentioned before, post hoc tests are needed after ANOVA in order to detect where the significant differences are.In this study, post hoc test with Bonferroni corrections was applied within ANOVA in SPSS for the behavioral data. Bonferroni correction is a correction for multiple comparisons which decreases the alpha level of significance. This level is defined by the equation 3.14 The disadvantage is that Bonferroni correction is a strict method when multiple comparisons are included [54].

$$\alpha_B = \frac{\alpha_{FWE}}{c} \tag{3.14}$$

where α_{FWER} is the familywise error rate and c is the number of comparisons.

Experiment 4

4.1 Pilot study

A pilot study was conducted before the real experiment to investigate the design and feasibility of the methods and procedures. Two participants took part in the pilot study which was enough to collect data for a preliminary analysis. The pilot study helped to detect some problems which were fixed in order to proceed to the real experiment.

The first problem that occurred during the pilot was occasional disconnection of the EEG cap. The problem was solved by checking the connectivity of all the electrodes on the cap and finally replacing the Cz- electrode, which created the problem, by a new one. Another encountered complication during the pilot study was that the triggers created by the stimulation software were delayed in the EEG recording window. To obtain time-locked events the EEG hardware was connected to the stimulator software through a DAQ-board. Every time a stimulation occurred, a trigger (trigger 5) was displayed in the EEG recordings which had a specific artefact to indicate the moment of the stimulation (an example of trigger 5 display is shown in figure 4.1). This artefact appeared with a delay at some random time points of the recordings. To fix this problem all the settings for each device were checked and the trigger files were modified in the stimulation software. After this inspection, the problem did not appear again, however precautions were taken during the next few recordings to track if the problem still existed.

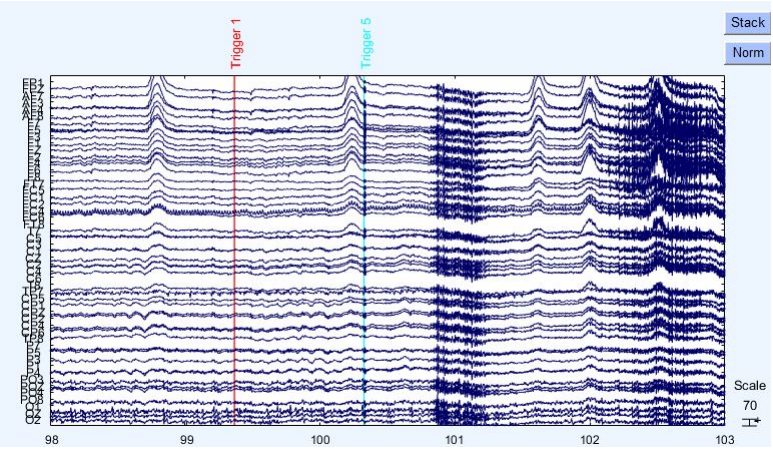

Figure 4.1: *This is an example of an EEG dataset during the pilot study. Time-locked events were indicated by 'Trigger 5' in the EEG recordings. Additionally, 'Trigger 1' indicated the intensity of the stimulation (1=Low, 2=High)*

During the pilots, the stimulation procedure consisted of 3 different intensities and was divided in 2 blocks and each block included 30 stimulations in a randomized order of intensity. However the obtained sample size for every stimulation intensity was too small for further analysis. Due to this, it was decided to have 2 different intensities per block instead of 3, resulting in a bigger number of trials (30) for each intensity. This is not only beneficial for independent component analysis (ICA), but it also helps to obtain a more clean average ERP than those with few repetitions . The decision of reducing the number of intensities was made instead of making a new block of stimulation, because more blocks might create habituation and sensitization to the electrical stimulation and would prolong the experiment which could be too tiring for the participants.

A preliminary analysis was made to evaluate the statistical variability of the data and for the researchers to get familiarized with the procedures and steps of the EEG data analysis.

4.2 Experimental Set-up

The full experimental set-up consisted of three technical parts: the mixed reality system, the electrical stimulation equipment and the EEG recording devices. The procedure consisted of three conditions: control, illusion, and covered which appeared in a counterbalanced order. The experimental set-up for the control and illusion conditions is shown below in figure 4.2 and the participants' view from the mixed reality system is shown is figure 4.3. The experimental protocol can be found in Appendix II.

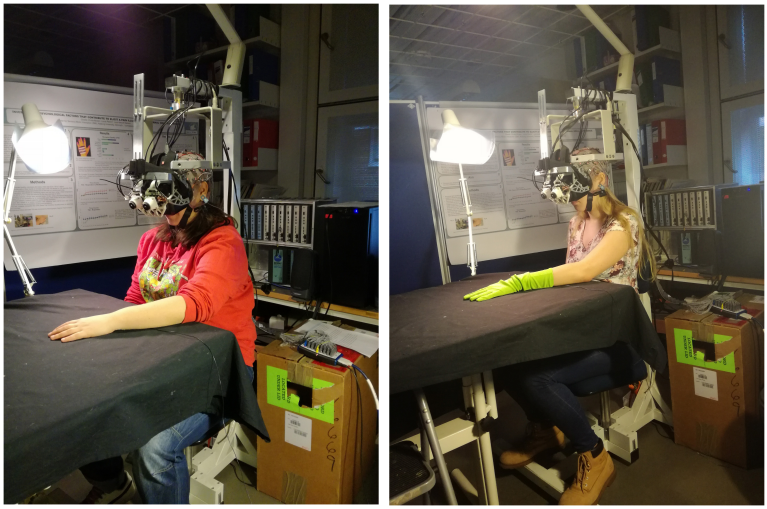

Figure 4.2: *The experimental set-up for 2 conditions. The figure on the left shows the set-up during the control condition and the figure on the right during the illusion condition.*

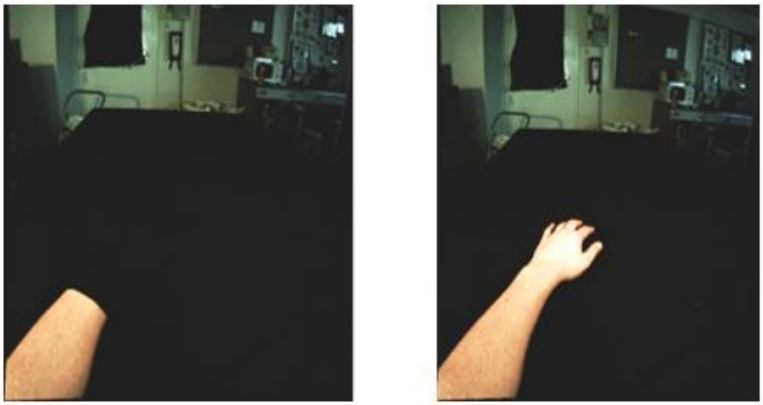

Figure 4.3: *The participants' view from the mixed reality system. On the left it shows the illusion from the participants' perspective and on the right is the view they had during the control illusion [12].*

Results 5

5.1 Behavioral results

5.1.1 Proprioceptive drift

There were three measurements at the end of each condition for each measured point (tip of the index finger, knuckle, wrist and stimulus location), which then were averaged for statistical analysis. The means and standard deviation were calculated for each measured point and every condition and they are reported in table 5.1 (all measures are in cm). The sign of the values indicates the direction of the drift. Particularly, '+' means that the measurement was below to the actual position meaning more proximal to the body and '-' means that it was above meaning more distal. A one-way ANOVA with repeated measures was performed for each reference point among conditions. There were significant differences in the following: Tip of the index finger (F(2,38)=9.409, p=0.000), knuckle (F(2,38=3.82, p=0.031)) and the location of stimulation (F(2,38)=4.706, p=0.015) showed significant difference. The tables 5.2, 5.3, 5.4, 5.5 show the averaged values for each measure point and each condition among 20 subjects. Each PD measure was calculated as a difference between the actual position of the measured point and the position determined by the participants. To calculate this difference the equation 5.1 was used

$$\Delta = \text{ ActualPosition - PerceivedPosition = (RefPoint + DistanceRef) - ParticipantPosition} \quad (5.1)$$

where ActualPosition is the actual position of the measured point, PerceivedPosition is the position of measure point determined by participant, RefPoint is the reference point located in the 37th cm of the ruller and DistanceRef is the distance measured from the reference point to the actual position of the measured point. An example of calculation is given below 5.2.

$$\text{example}\Delta = (37 - 3) - 28 = 6 \text{ cm} \quad (5.2)$$

Table 5.1: *Averaged values of the proprioceptive drift with standard deviation for each measured point of PD measurement in each condition.*

Condition	Index finger [mean ± SD (cm)]	Knuckle [mean ± SD (cm)]	Wrist [mean ± SD (cm)]	Stimulus [mean ± SD (cm)]
Control	4.2 ± 3.5	0.7 ± 3.9	-3.0 ± 4.2	-0.4 ± 4.2
Illusion	7.8 ± 4.7	3.2 ± 4.5	-1.7 ± 4.5	2.3 ± 5.5
Covered	6.2 ± 3.9	2.3 ± 4.4	-2.0 ± 4.5	0.9 ± 4.7

Table 5.2: *The averaged PD measurements categorized by condition for Tip of the index finger.*

	Proprioceptive drift (cm)		
No. Sub	Control	Illusion	Cover
1	7	12	7
2	0.5	7.5	1
3	4	11	5.5
4	1	4.5	3
5	6	8	7
6	6	4	2
7	0.5	8	3.5
8	2.5	5	6
9	12.5	11.5	14
10	-1.5	-2.5	10
11	-0.5	-0.5	1
12	3	8	1.5
13	6.5	16	11
14	7	7.5	5
15	8.5	12	10
16	1	2.5	2
17	6.5	12	11.5
18	4	9	10.5
19	6.5	13.5	6
20	2	6	6

Table 5.3: *The averaged PD measurements categorized by condition for the knuckle.*

	Proprioceptive drift (cm)		
No. Sub	Control	Illusion	Cover
1	1.5	8.5	2.5
2	-2.5	2.5	-5
3	2.5	6.5	3.5
4	-2	3	2.5
5	2.5	5.5	1.5
6	3	2.5	0
7	5	3	-1
8	-4.5	-1	1
9	9.5	5.5	10
10	-1	-2	6
11	-6.5	-8	-5.5
12	0.5	4	-3
13	4	12.5	8
14	4	1.5	3
15	1.5	5.5	4.5
16	-4	-3	-2
17	2.5	6	7
18	-2.5	1.5	9
19	3	7.5	1.5
20	-2.5	1.5	1.5

Table 5.4: *The averaged PD measurements categorized by condition for the wrist.*

	Proprioceptive drift (cm)		
No. Sub	Control	Illusion	Cover
1	-2	1	-6
2	-7.5	-2.5	-8.5
3	2	5.5	3
4	-4.5	0	0
5	0	3	2.5
6	-0.5	-2.5	-2
7	-7.5	-4	-5.5
8	-5.5	-5	-1.5
9	7	-3	4
10	-4	-6	2
11	-11	-11.5	-11
12	-1	-3	-6.5
13	0.5	8	3
14	-3	-2	-3.5
15	-1	-1	-1.5
16	-9	-8	-8
17	-1	0.5	3
18	-6	-3	2
19	-0.5	3.5	-2
20	-4.5	-3	-3.5

Table 5.5: *The averaged PD measurements categorized by condition for the stimulus location.*

	Proprioceptive drift (cm)		
No. Sub	Control	Illusion	Cover
1	4.5	8	6.5
2	-1	0	-6
3	3.5	5.5	5
4	-3	2.5	0.5
5	-1	13.5	7
6	3	1.5	0
7	-5	0	-5
8	0.5	-2.5	0
9	5	7	6.5
10	-1	-5	1.5
11	-6	-2.5	-5.5
12	-2.5	-5.5	-4.5
13	6	4	4.5
14	0	3	5
15	4	11	7.5
16	-10.5	-3.5	-5
17	-2.5	4	4.5
18	-2.5	-0.5	-1
19	3	9.5	-1.5
20	-3	-4	-2

5.1.2 Subjective pain ratings

The subjective pain ratings were averaged by the equation 5.3 for all the subjects and categorized by condition, for both intensities (low and high) of stimulus as it is shown in tables 5.6 and 5.7. The two-way repeated measures ANOVA performed on the intensity of perception of nociceptive stimuli did not show significant main effects among the three conditions ($F(2,0.147) = 0.864$, $p < 0.05$). However, it showed significant differences between the two different intensities ($F(1,75.158) = 0.000$, $p < 0.05$). Additionally, a three-way ANOVA was also performed with the factors condition ($F(2,0.052) = 0.949$, $p < 0.05$), intensity ($F(1,65.1) = 0.000$, $p < 0.05$) and gender ($F(1,2.384) = 0.126$, $p < 0.05$) but it showed no significant difference on the pain perception. The results of the two-way ANOVA test are shown in figure 5.1.

$$\mu = \frac{x_1 + x_2 + \cdots + x_n}{n}, \tag{5.3}$$

where x_1 is the rating for the first trial, x_2 is the rating from the second trial and n is the total number of trials for each intensity, here it was n = 30.

Table 5.6: *The averaged pain ratings (VAS scores) for the low-intensity stimulation categorized by condition*

Subjective Pain Ratings			
No. Subject	Control	Illusion	Covered
1	1	0.5	2.5
2	1.5	2	1.5
3	1	0.5	0.5
4	2	2	3
5	1	1	0.5
6	0.5	0.5	1
7	3.5	2	3
8	1.5	0	0.5
9	1.5	2	1
10	1.5	1	1
11	1.5	1	2.5
12	1.5	1.5	1
13	2	1.5	2
14	1	1.5	1
15	1.5	1	1.5
16	0	0	0
17	2.5	1.5	1.5
18	0	2.5	1.5
19	1	1.5	1
20	1.5	2.5	1

Table 5.7: *The averaged pain ratings (VAS scores) for the high-intensity stimulation categorized by condition*

Subjective Pain Ratings			
No. Subject	Control	Illusion	Covered
1	1.5	2.5	2.5
2	2.5	2.5	2
3	1.5	1.5	2.5
4	3	3.5	4.5
5	3	2	3.5
6	1	1	2
7	5.5	6	5.5
8	3.5	2.5	2.5
9	4.5	5	4
10	4	4	2.5
11	3.5	3	3
12	2	2.5	1.5
13	4.5	3	4.5
14	2	1.5	2
15	3.5	3.5	3.5
16	1	1	1
17	3	2.5	2.5
18	5	1.5	2
19	2	3	2
20	4.5	5	4

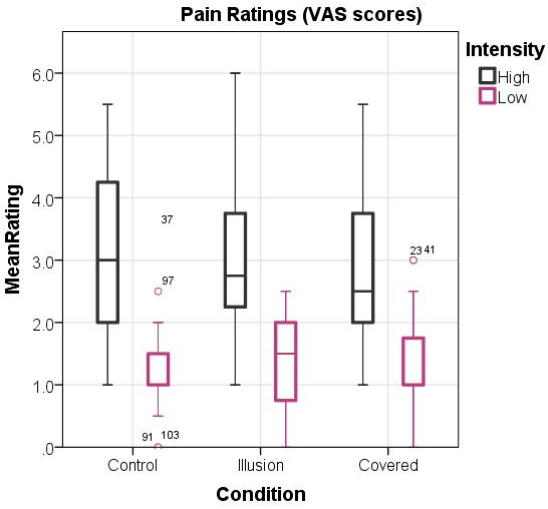

Figure 5.1: *The plot shows the averaged values of subjective pain ratings for each condition for both intensities.*

5.2 Electrophysiological results

5.2.1 Event related potentials (ERPs)

For each experimental condition and each participant ERPs where collected from all the connected electrodes during electrical stimulation. Below, the results are presented for every condition and for particular electrodes in waveforms and in scalp maps. For the both presented forms, the averaged activity for the high-intensity stimulation is displayed.

5.2.1.1 Control and Illusion

The control and illusion conditions showed significant differences at the following electrodes: C2, C6, FC5, CP1, CPz, CP2, CP4, CP6, P1, Pz, P2, P4, P6, POz, PO4. The test was made only for the high-intensity stimulation and the electrodes with the significance difference are shown in figures 5.2, 5.3, 5.4, 5.5. Additionally, the topographic maps are shown in figure 5.6 along with the significant differences between the conditions.

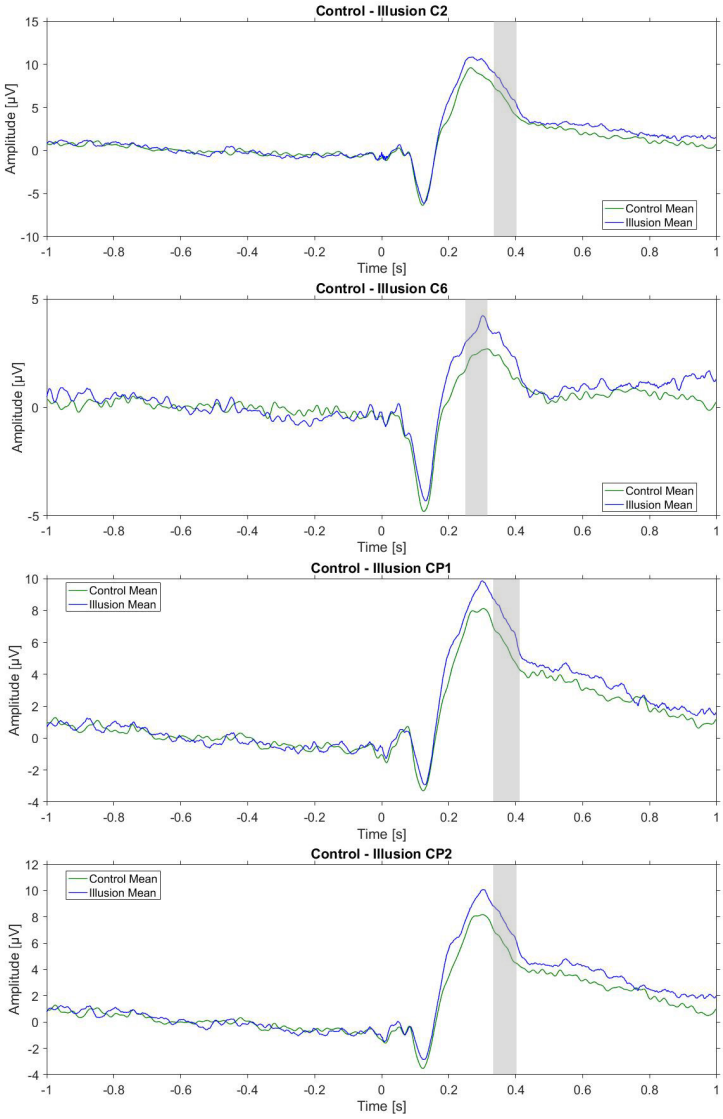

Figure 5.2: *Averaged ERPs compared for control and illusion, only for high-intensity stimulation for the following electrodes: C2, C6, CP1, CP2. The shading area in the plot indicates where the significant difference occurred between the two conditions.*

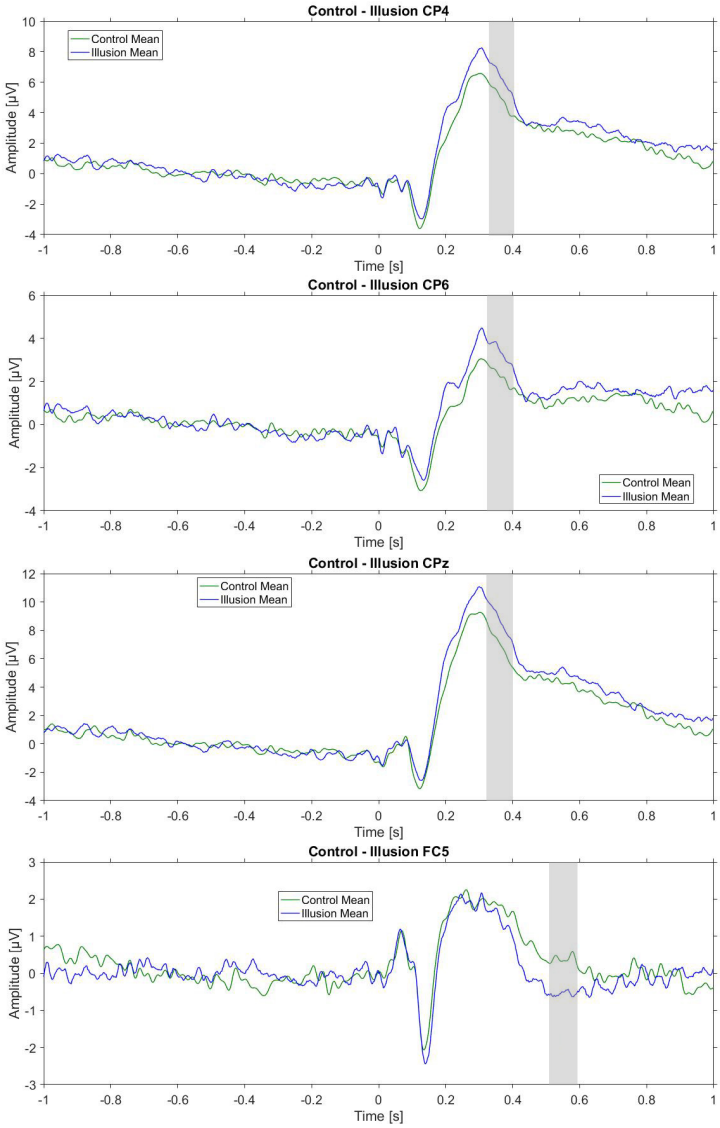

Figure 5.3: *Averaged ERPs compared for control and illusion, only for high-intensity stimulation for the following electrodes: CP4, CP6, CPz, FC5. The shading area in the plot indicates where the significant difference occurred between the two conditions.*

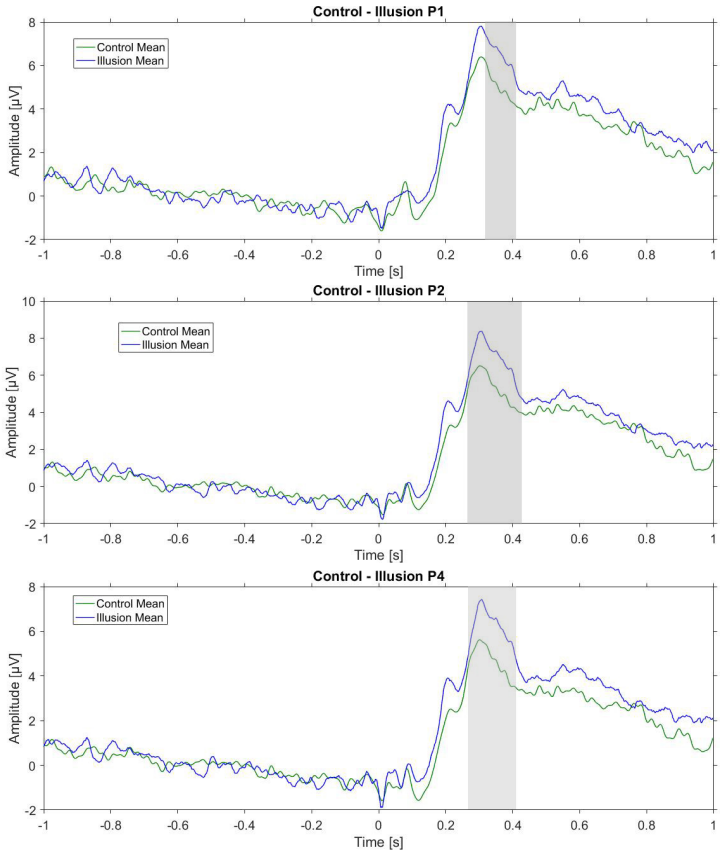

Figure 5.4: *Averaged ERPs compared for control and illusion, only for high-intensity stimulation for the following electrodes: P1, P2, P4. The shading area in the plot indicates where the significant difference occurred between the two conditions.*

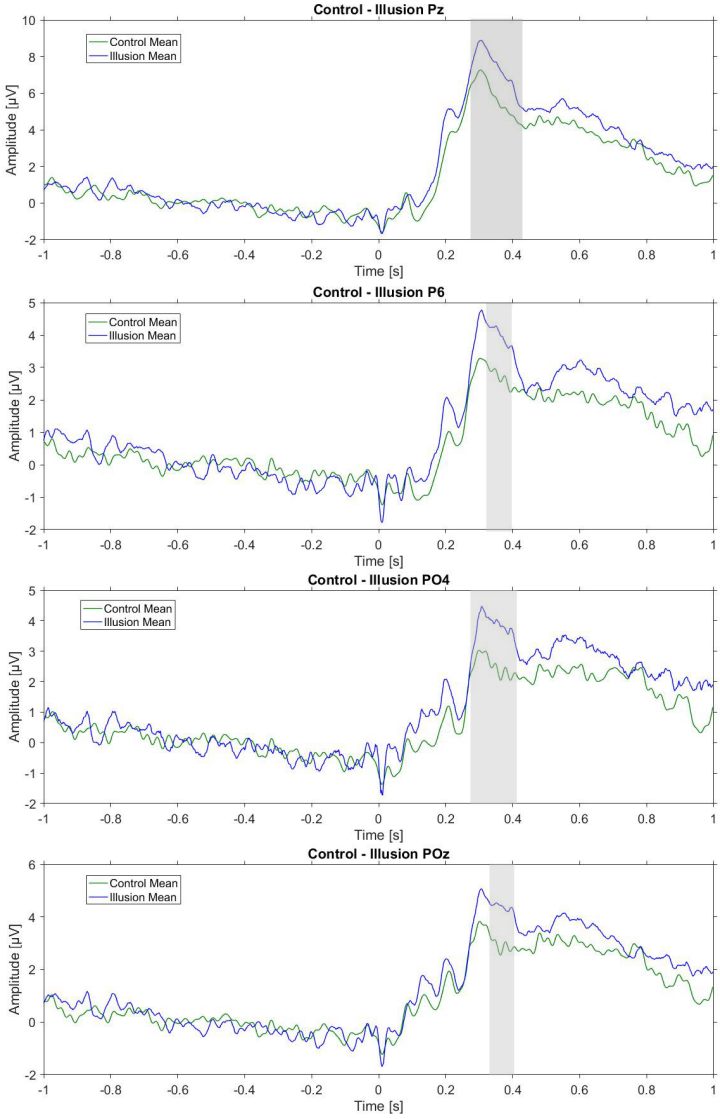

Figure 5.5: *Averaged ERPs compared for control and illusion, only for high-intensity stimulation for the following electrodes: Pz, P6, PO4, POz. The shading area in the plot indicates where the significant difference occurred between the two conditions.*

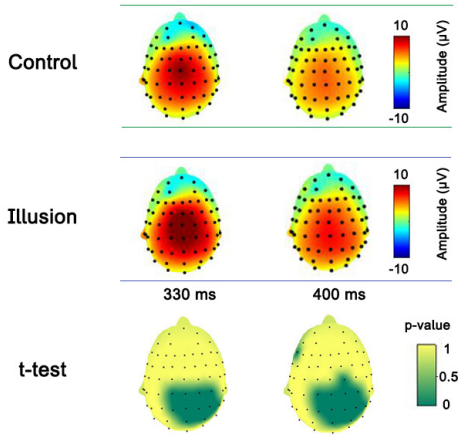

Figure 5.6: *Topographies of the averaged ERPs between control and illusion conditions at 330 ms and 400 ms. For each t-test the significant difference is showed in the last row. The different time points were selected from the significance range.*

5.2.1.2 Control and Covered

The control and covered conditions showed significant differences at the PO8 and Oz electrode. The test was made only for the high-intensity stimulation and the electrodes with the significance difference are shown in figure 5.7. Additionally, the topographic maps are shown in figure 5.8 along with the significant differences between the conditions.

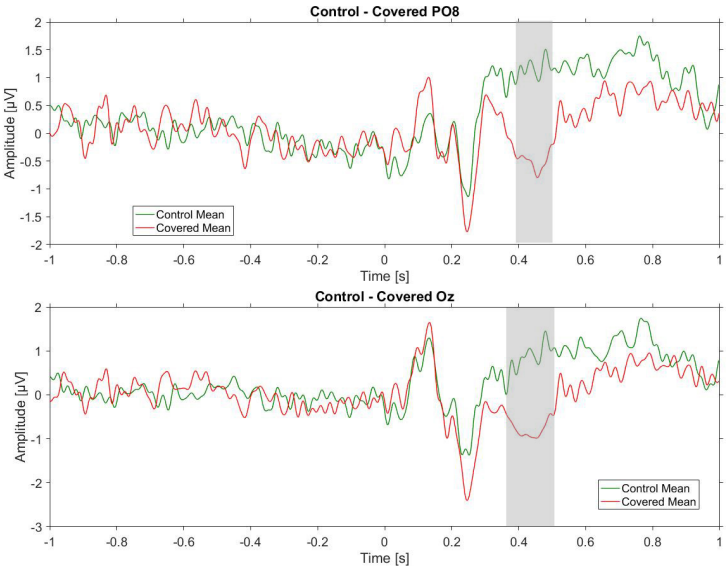

Figure 5.7: *Averaged ERPs compared for control and covered condition, only for high-intensity stimulation for the following electrodes:PO8 and Oz. The gray shading on the plots indicates where the significant difference occurred between the conditions.*

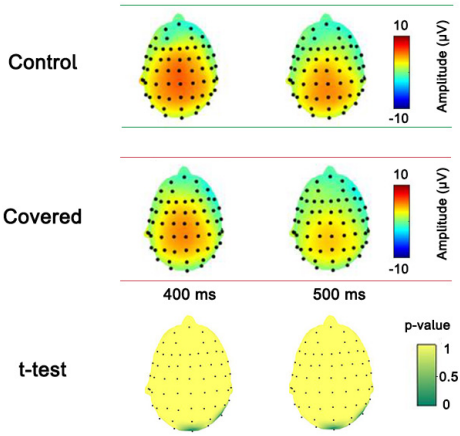

Figure 5.8: *Topographies of the averaged ERPs between control and covered conditions at 400 ms and 500 ms. For each t-test the significant difference is showed in the last row. The different time points were selected from the significance range.*

5.2.1.3 Illusion and Covered

The illusion and covered conditions showed significant difference in the following electrodes: Cz, CPz, CP2, CP4, Pz, P2, P4, P6, PO3 and POz. The test was made only for the high-intensity stimulation and the electrodes with the significance difference are shown in figures 5.9, 5.10, 5.11. Additionally, the topographic maps are shown in the figure 5.12 along with the significant differences between the conditions.

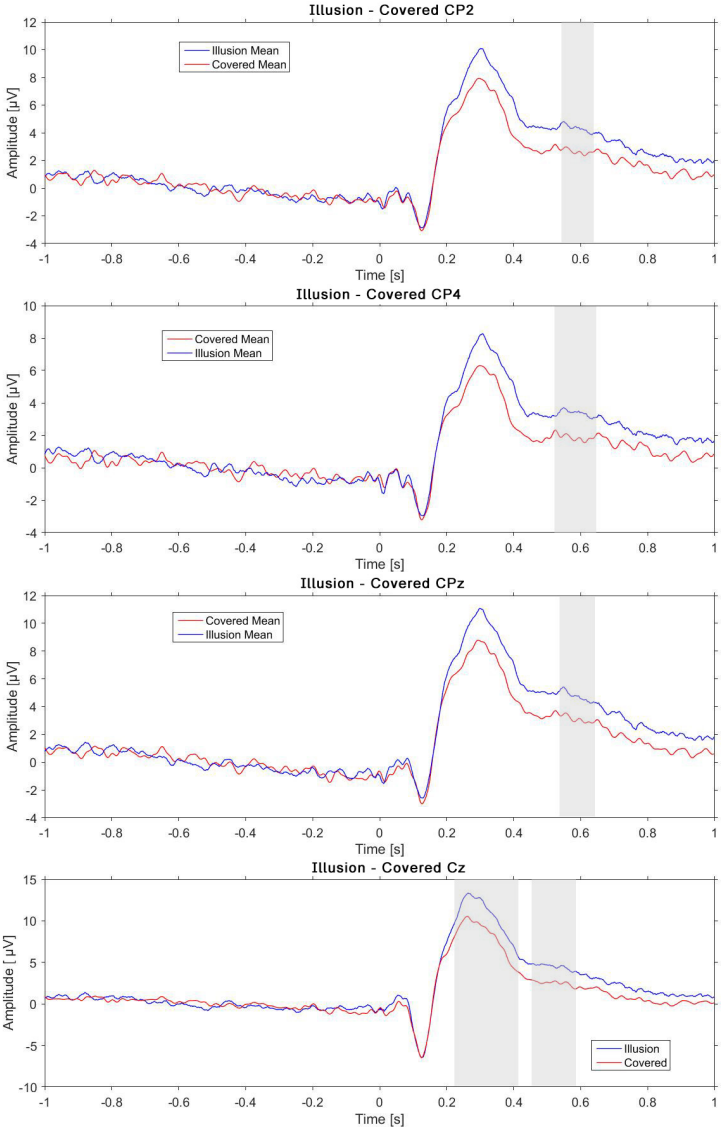

Figure 5.9: *ERPs compared for illusion and covered conditions for the following electrodes: CP2, CP4, CPz and Cz only for high-intensity stimulation. The gray shading on the plots indicates where the significant difference occurred between the conditions.*

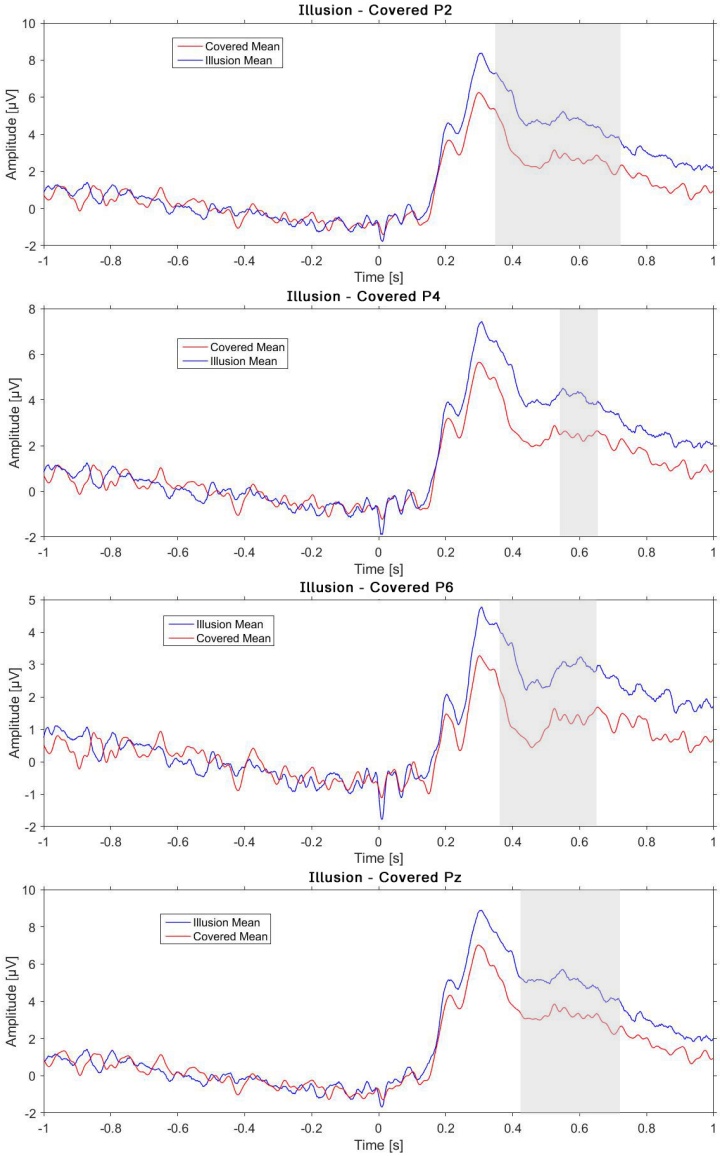

Figure 5.10: *ERPs compared for illusion and covered conditions for the following electrodes: P2, P4, P6 and Pz. The gray shading on the plots indicates where the significant difference occurred between the conditions.*

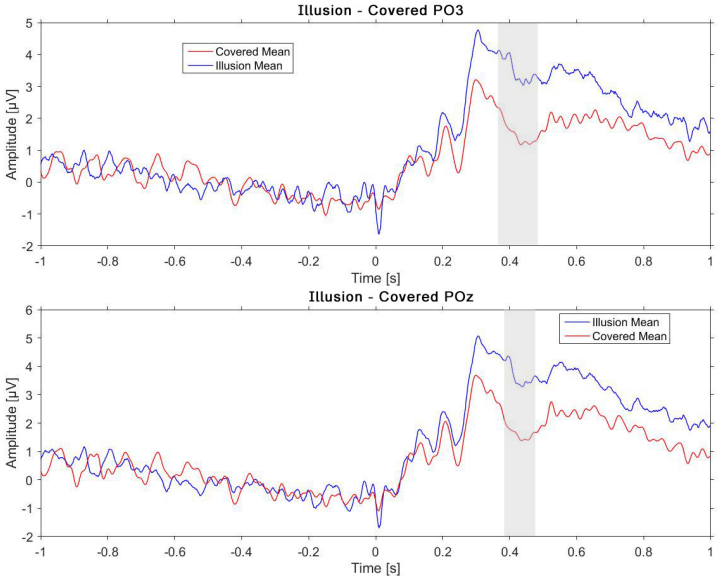

Figure 5.11: *Averaged ERPs compared for illusion and covered conditions for the following electrodes: PO3 and POz. The gray shading on the plots indicates where the significant difference occurred between the conditions.*

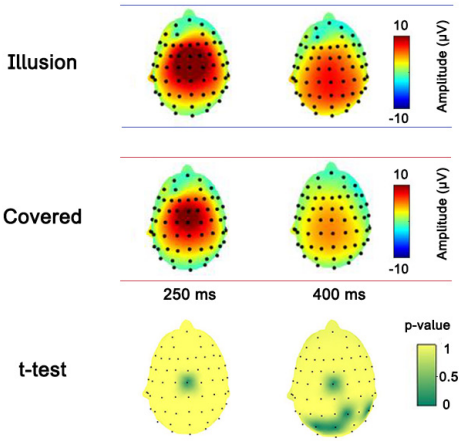

Figure 5.12: *Topographies of the averaged ERPs between illusion and covered conditions at 250 ms and 400 ms. For each t-test the significant difference is showed in the last row. The different time points were selected from the significance range.*

6 Discussion

6.1 Behavioral Data

6.1.1 Proprioceptive drift

The averaged values for the proprioceptive drift show that the drift is the highest during the illusion condition for all measured points, besides the wrist. This indicates that the illusion influenced the proprioception and the ability of spatial localization of own body parts. Moreover, the sign of the averaged values indicates the direction of the drift. All of them show that there is a positive drift during conditions, meaning that the participants, in average, reported the measure point below its actual position meaning more proximal to their body. The exception is again the wrist, where in all conditions the drift has negative sign. This sign of the averaged value was also the same when the participants localized the stimulus in the control condition. The negative sign indicates that the reported position was above the actual position of the measured point meaning more distant to the body. These results are compatible with the ones from Thøgersen et al. where the wrist was localized with equal precisions between control and illusion conditions, possibly due to the fact that it was the closest part of the body that the participants could see [12]. The current results indicate that the participants perceived their limb shorter than it actually was. Moreover, the results of Schaefer et al. 2007 suggested that perceived changes in the size of body parts may be related to temporal functional changes in SI [15]. Therefore, the proprioceptive drift during the illusion may indicate the involvement of SI. This involvement of SI has also been discussed in the study of Flor et al. 2006 where it was suggested that there is reorganization of SI in PLP patients [2]. However, the current study shows that this can also be observed in healthy participants suggesting that the bias of body-awareness in PLP patients is related also to faulty update of body schema rather than the nerve damage alone.

6.1.2 Subjective pain ratings

The results for the subjective pain ratings show that the three different conditions did not have any significant effect on the perception of pain. No significant difference observed may be caused because

the participants were not trained before the experimental sessions. Moreover, the inclusion criteria for the study did not define that they should have previous experience with pain experiments. Between the two intensities of stimulation there was a significant difference, which was expected. The extra test that was conducted with the added factor gender, showed again only significant difference between the two intensities. This was done because it has been proved that there are gender differences on pain threshold and tolerance [55] and also PLP is reported to be more common in women [56].

6.2 Electrophysiological Data

The electrodes where the significant differences were found indicate that the effect of the illusion was mainly within the parietal lobe, in primary somatosensory area at the contralateral side of the left hand. This shows that the conditions differed mostly in regards to sensory processing and integration of visual and proprioceptive inputs. Moreover, the parietal lobe is suggested to be involved in egocentric spatial awareness beyond the field of view. The illusion seems to have affected spatial identification of the parts of the participants' own body, which extents the possibility that parietal functions not only include external space representation but also personal space. It was suggested that posterior parietal cortex is responsible for maintaining a representation of the body image previously mentioned as body schema [57].

6.2.1 Control vs Illusion

The significant difference observed, between control and illusion, is in a range between 250 and 420 ms for all ERPs, except the one recorded at the electrode FC5 which is in a range of 500 to 600 ms. The former range is within the P2-wave, which indicates that the sensory processing differs between these two conditions. However, the latter range is after the P2-wave. The ERP recorded at this electrode has the lowest amplitude of the reported ones around 2 μV and the channel is noisy. It can be debated that the significant difference found in this electrode might not be observed because of the illusion, but it can be caused by not optimal signal processing procedure on the low amplitude datasets. Furthermore, the topographic maps between the two conditions show that there was an increased brain activity during the illusion condition compared to the control at the latencies within the significance range. Additionally, the amount of electrodes and their spatial distribution that contributes to the significant difference (figure 5.6) shows in concurrence with the ERP plots, that there was a large effect of the illusion on cortical responses.

6.2.2 Illusion vs Covered

All electrodes showed significant difference, between illusion and covered conditions, after the P2-wave in the range around 380 to 700 ms. As discussed in the chapter 3 there is an essential difference between the nociceptive and tactile ERPs, when in the first one the response is more sharp and slower compared to the second. Some of the plots show the appearance of small early responses before the N1-wave, which represents the detection response. This indicates that tactile fibres were activated, which was not intended with the current stimulating method.
Moreover the topographic maps showed enhanced activity in the illusion condition in the central area, especially at 400 ms. However, the t-test showed a limited number of electrodes contributing in the significant difference between the two conditions. Particularly, at 250 ms it seems that there is only one

electrode present in this topographic map, whereas in the second map at 400 ms there is, additionally to this electrode, more activity in the parietal lobe. This leads to the assumption that not all the channels were optimally processed. Based on this assumption the datasets were rechecked for outliers. After removing the outlier another t-test was conducted on the new dataset, which showed significant differences in a reduced number of electrodes. In details, there was no significant differences among CPz, P6, POz and PO3 electrodes. These two conditions intended to reflect the absence of visual feedback in different ways. Apparently, the illusion condition induced an altered cortical response in contrast to the covered which did not differ substantially from the control condition.

6.2.3 Control vs Covered

The number of electrodes where there were significant differences between the two conditions, is two. The range of the shading area is between 380 and 500 ms which is outside the ERP components. These indicate that the two conditions might not be that different eventually. This observation resulted in a post process check of the datasets which showed that the significant differences might be caused because of an outlier. In agreement with the above, the topographic maps between the two conditions showed limited contribution to the significant differences and similar brain activity.
After removing the outlier, another t-test was conducted to the new datasets, which showed significant differences only on Oz electrode. The ERPs had again a low amplitude and the range of the significant difference was between 400 and 500 ms which is outside of the ERP components. This indicates that it can be a result of not optimal signal processing procedure.
The topographic maps show low activity in the two conditions, however it can be noticed that the activity is enhanced during control compared to covered condition. This stays in contrast with our hypothesis and with the previous findings that not seeing the part of the body increases pain perception. Nevertheless, the opposite results can be influenced by the set-up of the covered condition, where a soft towel was used to cover the hand and the forearm. The towel was touching the participants' body directly and by this, it is possible that non-nociceptive fibres were elicited. Corresponding to the gate-control theory of pain proposed by Melzack and Wall in 1965, the stimulation of non-nociceptive fibres along with the stimulation of nociceptive fibres can affect and inhibit the transmission of the latter ones. The inhibition is suggested to act through the inhibitory interneurons in the dorsal horn of the spinal cord, influencing the projection neurons in the cortex. The inhibitory interneurons act as a gate which either allows the nociceptive signals to be transmitted to the cortex or suppresses them. The suppression is only possible when there is an input to the inhibitory interneurons from non-nociceptive fibres [58]. A diagram presenting the two above mentioned situations is shown in figure 6.1.

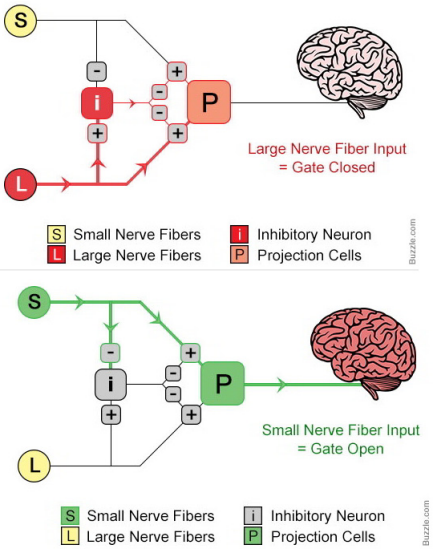

Figure 6.1: *Illustration of gate-control theory. The exclusive input from nociceptors opens the gate. The non-nociceptive input closes the gate.*

After neurophysiology investigations in animals the theory was complemented with the presence of wide-dynamic range neurons (WDR neurons) with a particular receptive field (RF), which are homologue with projection neurons and/or interneurons proposed by Melzack and Wall. These neurons are mulitmodal, which means that they respond to both non-nociceptive and nociceptive inputs. Their RF has a structure of an excitatory center and peripheral inhibitory surroundings. It has been shown that a tactile stimulus within the inhibitory field and on the periphery of this field could reduce pain perception [59].
Besides the gate-control theory, Inui et al. 2005 have shown that the inhibitory effect is present on the cortical level, when applying both nociceptive and vibrotactile stimulation. Particularly, this study has shown that even when the signals from both tactile and nociceptive fibres arrive asynchronously to the spinal cord there is still the inhibitory effect seen in the cortical activity [60]. However, the inhibitory mechanisms are not the certain cause of the effect on ERPs during covered condition. After this debate, a suggestion was made that the covered condition should include the use of an object which would not touch the body of the participants directly, i.e a box.

6.3 Saliency detection

This study intended to elicit nociceptive specific fibers with the use of the CPE. The study of Lelic et al. 2011 has shown that this electrode can selectively elicit nociceptive fibers with low intensity stimulation [50]. However, the results of this study indicate that it is possible that the stimulating method was not entirely nociceptive specific based on the observation of early ERP components (around 50 ms).

Additionally, from the range of averaged values (VAS scores 1-6 for the high-intensity stimulation) of the subjective pain ratings it can be seen that not every stimulation was reported by the participants as painful. Taken together, the incoherence between the cortical responses and subjective pain ratings indicate that the observed brain activity can reflect salient stimulus processing regardless the modality of stimulation [61–63]

Bibliography

[1] B. Subedi and G. T. Grossberg, "Phantom limb pain: Mechanisms and treatment approaches," *Pain Research and Treatment*, 2011.

[2] H. Flor, L. Nikolajsen, and T. Jensen, "Phantom limb pain: a case of maladaptive cns plasticity?," *Neuroscience*, 2006.

[3] S. Griffin and J. Tsao, "A mechanism-based classification of phantom limb pain," *Pain*, 2014.

[4] E. Kalso, J. Loeser, B. Dickinson, A. Head, S. Gitlow, and A. Osbahr, "Maldynia: Pathophysiology and management of neuropathic and maladaptive pain," *Pain Medicine*, 2011.

[5] S. Weeks, V. Anderson-Barnes, and J. Tsao, "Phantom limb pain: theories and therapies," *Neurologist*, 2010.

[6] Y. Oouchida and S. Izumi, "Imitation movement reduces the phantom limb pain caused by the abnormality of body schema," *International Conference on Complex Medical Engineering*, 2012.

[7] S. Das, Y. Yuan, and H. Yang, "Neuroimaging: A key unlocking phantom limb pain," *Austin Neurology & Neurosciences*, 2016.

[8] V. Ramachandran, D. Rogers-Ramachandran, and M. Stewart, "Perceptual correlates of massive cortical reorganization," *Science*, 1992.

[9] R. Melzack, "Pain and the neuromatrix in the brain," *Journal of Dental Education*, 2001.

[10] H. Head and G. Holmes, "Sensory disturbances from cerebral lesions," *Brain*, 1911.

[11] P. Haggard and D. Wolpert, "Disorders of body scheme," *Higher-Order Motor Disorders, Ed. Freund, Jeannerod, Hallett & Leiguarda, Oxford University Press*, 2005.

[12] M. Thø gersen, J. Hansen, L. Arendt-Nielsen, H. Flor, and L. Petrini, "A visual feedback system using mixed reality to simulate a phantom limb illusion in healthy volunteers," *Unpublished manuscript*, 2017.

[13] L. Chen, R. Friedman, and A. Roe, "Optical imaging of a tactile illusion in area 3b of the primary somatosensory cortex," *Science*, 2003.

[14] L. Egsgaard, L. Petrini, G. Christoffersen, and L. Arendt-Nielsen, "Cortical responses to the mirror box illusion: a high-resolution eeg study," *Experimental Brain Research*, 2011.

[15] M. Schaefer, H. Flor, H. Heinze, and M. Rottea, "Morphing the body: Illusory feeling of an elongated arm affects somatosensory homunculus," *NeuroImage*, 2007.

[16] M. Longo, G. Iannetti, F. Mancini, J. Driver, and P. Haggard, "Linking pain and the body: Neural correlates of visually induced analgesia," *Journal of Neuroscience*, 2012.

[17] M. Longo, V. Betti, S. Aglioti, and P. Haggard, "Visually induced analgesia: Seeing the body reduces pain," *The Journal of Neuroscience*, 2009.

[18] F. Mancini, M. Longo, M. Kammers, and P. Haggard, "Visual distortion of body size modulates pain perception," *Psychological Science 22*, 2011.

[19] B. Chan, R. Witt, A. Charrow, A. Magee, R. Howard, P. Pasquina, K. Heilman, and J. Tsao, "Mirror therapy for phantom limb pain," *The New England Journal of Medicine*, 2007.

[20] M. Sumitani, S. Miyauchi, C. McCabe, M. Shibata, L. Maeda, Y. Saitoh, T. Tashiro, and T. Mashimo, "Mirror visual feedback alleviates deafferentation pain, depending on qualitative aspects of the pain: a preliminary report," *Rheumatology (Oxford)*, 2008.

[21] S. Kim and Y. Kim, "Mirror therapy for phantom limb pain," *The Korean Journal of Pain*, 2012.

[22] M. Botvinick and J. Cohen, "Rubber hands 'feel' touch that eyes see," *Nature*, 1998.

[23] K. Armel and V. Ramachandran, "Projecting sensations to external objects: evidence from skin conductance response.," *Proceedings Biological Sciences*, 2003.

[24] D. Torta, V. Legrain, and A. Mouraux, "Looking at the hand modulates the brain responses to nociceptive and non-nociceptive somatosensory stimuli but does not necessarily modulate their perception," *Psychophysiology, 52*, 2015.

[25] A. Karl, N. Birbaumer, W. Lutzenberger, L. Cohen, , and H. Flor, "Reorganization of motor and somatosensory cortex in upper extremity amputees with phantom limb pain," *The Journal of Neuroscience*, 2001.

[26] M. Teplan, "Fundamentals of eeg measurement," *MEASUREMENT SCIENCE REVIEW*, 2002.

[27] S. Sur and V. Sinha, "Event-related potential: An overview," *Industrial Psychiatry Journal 2009*, 2009.

[28] I. Stolerman and L. Price, eds., *Encyclopedia of Psychopharmacology*. Springer, 2015.

[29] W. Greffrath, U. Baumgartner, and R. Treede, "Peripheral and central components of habituation of heat pain perception and evoked potentials in humans," *Pain*, 2007.

[30] A. Wang, A. Mouraux, M. Liang, and G. Iannetti, "The enhancement of the 'n1' wave elicited by sensory stimuli presented at very short inter-stimulus intervals is a general feature across sensory systems," *PLoS One*, 2008.

[31] A. Runehov and L. Oviedo, eds., *Encyclopedia of Sciences and Religions*. Springer, 2013.

[32] A. Mouraux and D. Iannetti, G, "Brain responses to sensory stimuli are lalarge independent of sensory modality." Forum of European Neuroscience,, 2008.

[33] D. Senkowski and A. Heinz, "Chronic pain and distorted body image: Implications for multisensory feedback interventions.," *Neuroscience and biobehavioral reviews*, 2016.

[34] Jilani, ""difference between iir and fir filters."." DifferenceBetween.net. October 11, 2011, 2011. http://www.differencebetween.net/science/difference-between-iir-and-fir-filters/ >.

[35] W. Klonowski, "Everything you wanted to ask about eeg but were afraid to get the right answer," *Nonlinear Biomedical Physics*, 2009.

[36] A. Delorme, T. Sejnowskia, and S. Makeig, "Enhanced detection of artifacts in eeg data using higher-order statistics and independent component analysis," *NeuroImage*, 2006.

[37] A. Delorme and S. Makeig, "Eeglab: an open source toolbox for analysis of single-trial eeg dynamics including independent component analysis," *Journal of Neuroscience Methods 134*, 2004.

[38] G. Hawker, S. Mian, T. Kendzerska, and M. French, "Measures of adult pain: Visual analog scale for pain (vas pain), numeric rating scale for pain (nrs pain), mcgill pain questionnaire (mpq), short-form mcgill pain questionnaire (sf-mpq), chronic pain grade scale (cpgs), short form-36 bodily pain scale (sf-36 bps), and measure of intermittent and constant osteoarthritis pain (icoap)," *Arthritis Care and Research*, 2011.

[39] A. Wold, J. Limanowski, H. Walter, and F. Blankenburg, "Proprioceptive drift in the rubber hand illusion is intensified following 1 hz tms of the left eba," *Frontiers in Human Neuroscience*, 2014.

[40] P. Milgram and F. Kishino, "A taxonomy of mixed reality visual displays," *IEICE Transactions on Information Systems*, 1994.

[41] E. Dubois, P. Gray, and L. Nigay, *The Engineering of Mixed Reality Systems*. Springer, 2010.

[42] M. Martini, "Real, rubber or virtual: The vision of one's own body as a means for pain modulation. a narrative review," *Consciousness and Cognition 43*, 2016.

[43] D. Chandler and R. Munday, "A dictionary of media and communication." Published online, 2011.

[44] A. A. Battaglia, ed., *An Introduction to Pain and its relation to Nervous System Disorders*. John Wiley & Sons, 2016.

[45] M. Tommaso, R. Santostasi, V. Devitofrancesco, G. Franco, E. Vecchio, M. Delussi, P. Livrea, and Z. Katzarava, "A comparative study of cortical responses evoked by transcutaneous electrical vs co2 laser stimulation," *Clinical Neurophysiology*, 2011.

[46] R. Kakigia, K. Inuia, and Y. Tamuraa, "Electrophysiological studies on human pain perception," *Clinical Neurophysiology*, 2005.

[47] A. Mouraux, G. Iannetti, and L. Plaghki, "Low intensity intra-epidermal electrical stimulation can activate ad-nociceptors selectively," *PAIN*, 2010.

[48] J. Lefaucheur, R. Ahda, S. Ayache, I. Lefaucheur-Menard, D. Rouie, D. Tebbal, D. Neves, and D. Ciampi de Andrade, "Pain-related evoked potentials: A comparative study between electrical stimulation using a concentric planar electrode and laser stimulation using a co2 laser," *Neurophysiologie Clinique - Clinical Neurophysiology*, 2012.

[49] H. Kaube, Z. Katsarava, T. Kaufer, H. Diener, and E. J., "A new method to increase nociception specificity of the human blink reflex," *Clinical Neurophysiology*, 2000.

[50] D. Lelic, C. Mø rch, K. Hennings, O. Andersen, and A. Drewes, "Differences in perception and brain activation following stimulation by large versus small area cutaneous surface electrodes," *European Journal of Pain*, 2011.

[51] S. Shapiro and M. Wilk, "An analysis of variance test for normality (complete samples)," *Biometrika*, 1965.

[52] J. H. Jar, "Biostatistical analysis fifth edition," *Pearson*, 2010.

[53] E. Maris and R. Oostenveld, "Nonparametric statistical testing of eeg- and meg-data," *Journal of Neuroscience Methods*, 2007.

[54] T. Dickhaus, *Simultaneous Statistical Inference With Applications in the Life Sciences*. Springer, 2014.

[55] W. Hallin, "Sex differences in pain perception," *Gender Medicine*, 2005.

[56] H. Knotkova, R. Cruciani, M. Tronnier, and D. Rasche, "Current and future options for the management of phantom-limb pain," *Journal of Pain Research*, 2012.

[57] J. Stein, "Review article: Representation of egocentric space in the posterior parietal cortex," *Quarterly Journal of Experimental Physiology*, 1989.

[58] R. Melzack and P. Wall, "Pain mechanisms: A new theory," *Science*, 1965.

[59] F. Mancini, T. Nash, G. Iannetti, and P. Haggard, "Pain relief by touch: A quantitative approach," *Pain*, 2014.

[60] K. Inui, T. Tsuji, and R. Kakigi, "Temporal analysis of cortical mechanisms for pain relief by tactile stimuli in humans," *Cerebral Cortex*, 2005.

[61] I. Ronga, E. Valentini, A. Mouraux, and G. Iannetti, "Novelty is not enough: laser-evoked potentials are determined by stimulus saliency, not absolute novelty," *Journal of Neurophysiology*, 2013.

[62] G. Iannetti, "The electrocortical responses to nociceptive stimulation in humans," *Pain*, 2010.

[63] G. Iannetti, N. Hughes, M. Lee, and A. Mouraux, "Determinants of laser-evoked eeg responses: Pain perception or stimulus saliency?," *Journal of Neurophysiology*, 2008.

Part I

Appendix:

Table of detection threshold values and stimulation intensities

Table 6.1: *Detection threshold values along with calculation of the two intensities*

Subject No.	Detection Threshold [μA]	Low Intensity [μA]	High Intensity [μA]
1	135	270	540
2	110	220	440
3	170	340	510
4	110	220	440
5	270	540	1080
6	125	250	500
7	110	220	440
8	205	410	820
9	170	340	680
10	110	220	440
11	350	700	1400
12	100	200	400
13	205	410	820
14	110	220	440
15	190	380	760
16	170	340	680
17	180	360	720
18	125	250	500
19	140	280	560
20	112	224	448

Part II

Appendix:

Experimental Protocol

Participant no. Date:

EXPERIMENTAL PROTOCOL

The participant's personal data

Name	
Age	
Weight	
Height	
Number	

Mark which type of block are being done.

Condition A	Condition B	Condition C
Control	Illusion	Covered

Instructions

Nb	Task	Check
Before participant arrives		
1	Turn on the transformer	
2	Connect Analog output AO0 from the DAQ board to the input of the stimulator	
3	On the DAQ board connect from PF7 to P0.7 and the ground	
4	Form DAQ board connect Analog Input AI1 to the output of the stimulator	
5	Connect 1,2,3,4 pins from EEG to the DAQ board into P0.0 - P0.3	
6	Connect 5th pin as stimulus into PFI 13 in the DAQ board	
7	Connect the ground from EEG	
8	Connect VAS to AI0	
9	Connect EEG to the computer and power	
Camera computer		
10	Take out white HDMI cable before turning on the camera computer (the white one)	
11	One USB connect to the computer on the left	
12	Second USB connect on the top	
After participant arrives		
13	Proprioceptive drift measurement Measure the index finger and hand length Measure location of the slider for 3 points	
14	If the vision is not good for participant, measure IPD and change the settings for every subject (Tasks panel - HDMI - make new person - height and the eye measurement; Turn off and turn on camera again)	
15	Turn on Mr. Kick and load the trigger file (threshold file)	
Thresholds measurements for electrical stimulation		
16	Place the electrode	
17	Set the sensitivity in Mr. Kick which corresponds to the sensitivity of stimulator	
18	Run the trigger file with consecutive different intensities	
19	Write the mean value from Mr.Kick	
20	Multiply found threshold by a factor and put it in Mr. Kick. Save 3 different intensities for the stimulation.	

Participant no. Date:

EEG settings		
21	Measure the middle point of the inion and nasion and preauricular points	
22	Put Cz electrode in the measured middle point	
23	Secure the cap	
24	Put the reference electrode on the ear	
25	Connect the cables and turn on the g.Tec	
26	Turn on computer with g.Recorder	
27	Go to Mode > Administrator Mode > No password > Enter	
28	Measure the impedance (in g. Recorder go to Tools > Impedance measurement > Select group A > Start putting gel to the ground and 1st electrode)	
29	Select channels which we want to use and enable trigger (load the settings file)	
30	Settings > triggers> correspond them to the wires and name the to the class	
31	View > View data and press play to see the signal (To autoscale press loupe)	
32	Press red button to record	
Camera settings		
33	Put the participant into the chair and adjust height	
34	Place the camera and adjust screws	
35	Put the black material on the door	
36	Turn of the up lights	
37	Turn on the side lights	
38	Start UNITY	
39	If the is an error - restart computer	
40	Press play - it should run 2 screens	
41	Press M twice to get rid of the blue colour from the screens	
42	Press space to take the photo of the background (click the window view first)	
43	Press backspace to make a background disappearing	
Electrical Stimulation		
44	Load Mr. Kick settings	
45	Classes from the threshold measurement (multiply by a factor)	
46	Turn on the stimulator	
47	Start acquisition for block 1	
54	After every stimulation write the VAS rating	
55	After block 1 measure the stimulus location (give one stimulation more)	
56	Wait 1-2 minutes	
57	Start acquisition for block 2	
58	After every stimulation write the VAS rating	
59	After block 2 measure the stimulus location (give one stimulation more)	

Participant no. Date:

THRESHOLD MEASUREMENT:

Detection Threshold	Multiply by 1st factor	Multiply by 2nd factor

PROPRIOCEPTION MEASUREMENT:

Hand length: Finger length:

LOCATION	CON A.1	2	3	ref.	CON B.1	2	3	ref.	CON C. 1	2	3	ref.
Index												
Central												
Wrist												
Stim. Block 1												
Stim. Block 2												

VAS RATING:

CONTROL CONDITION				ILLUSION CONDITION				COVERED CONDITION			
BLOCK 1		BLOCK 2		BLOCK 1		BLOCK 2		BLOCK 1		BLOCK 2	
1		1		1		1		1		1	
2		2		2		2		2		2	
3		3		3		3		3		3	
4		4		4		4		4		4	
5		5		5		5		5		5	
6		6		6		6		6		6	
7		7		7		7		7		7	
8		8		8		8		8		8	
9		9		9		9		9		9	
10		10		10		10		10		10	
11		11		11		11		11		11	
12		12		12		12		12		12	
13		13		13		13		13		13	
14		14		14		14		14		14	
15		15		15		15		15		15	
16		16		16		16		16		16	
17		17		17		17		17		17	
18		18		18		18		18		18	
19		19		19		19		19		19	
20		20		20		20		20		20	
21		21		21		21		21		21	
22		22		22		22		22		22	
23		23		23		23		23		23	
24		24		24		24		24		24	
25		25		25		25		25		25	
26		26		26		26		26		26	
27		27		27		27		27		27	

Participant no. Date:

28		28		28		28		28		28	
29		29		29		29		29		29	
30		30		30		30		30		30	